

# Probing Conformational Fluctuation of Proteins by Pressure Perturbation

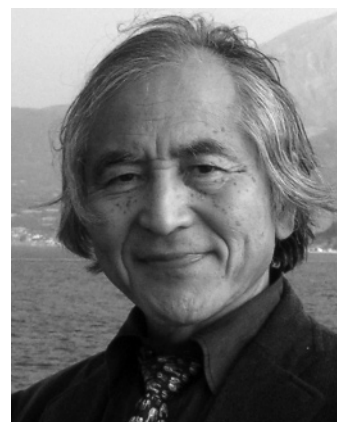
Kazuyuki Akasaka\*

School of biology-Oriented Science and Technology, Kinki University, 930 Nishimitani, Kinokawa-shi, Wakayama 649-6493, Japan, and Structural and Molecular Biology Laboratory, RIKEN Spring-8 Center, Harima Institute, 1-1-1 Kouto, Hyogo 679-5148, Japan

Received April 25, 2005

## Contents

1. Introduction	1814
2. Basic Rules Governing Pressure and Proteins	1815
2.1. Response of a Protein to Pressure	1815
2.2. General Compression within a Subensemble of Conformers	1816
2.3. Shift of Equilibrium between Different Subensembles of Conformers	1816
3. Experimental Techniques To Explore Pressure Effects on Proteins	1817
3.1. Established Techniques for General Compression and Global Conformational Changes	1817
3.2. High-Pressure NMR Technique for Site-Specific Conformational Changes	1818
4. Probing Fluctuations within the Folded Subensemble of Conformers	1820
4.1. Backbone Dynamics from Spin Relaxation	1820
4.2. Fluctuation from Pressure-Induced Shifts	1821
4.2.1. Fluctuation in Hydrogen Bonds	1821
4.2.2. Fluctuation in Tertiary Structure	1822
4.2.3. Time Range of Fluctuations Sensed by Pressure-Induced Shifts	1823
4.3. Infrequent Fluctuation of the Core Revealed from Ring-Flip Motions	1823
4.4. Fluctuation Involving Low-Lying Excited States (from Nonlinear Pressure Shifts)	1823
5. Probing Fluctuations Involving Transitions to Higher Energy Conformers	1825
5.1. Probing Fluctuations in a Wider Conformational Space—The Underlying Principle	1825
5.2. Application to Globular Proteins	1826
5.3. Kinetic Studies Using Pressure	1828
5.4. Close Identity of Kinetic Intermediates with Equilibrium Intermediates Stabilized by Pressure	1828
5.5. NMR “Snapshots” of a Fluctuating Protein Structure	1830
6. Fluctuations Involving Self-Association	1833
7. Conclusion	1834
8. Acknowledgment	1834
9. References	1834



Kazuyuki Akasaka was born in 1938 in Osaka (Japan) and received his bachelor's and master's degrees from Osaka University. In 1965, he received his Ph.D. degree in chemistry from Kyoto University, where he became a faculty member for about 20 years and began his research career in electron spin resonance of sulfur-containing amino acid crystals. After he spent a couple of years in North Carolina in the late 1960's as a Fulbright scholar, he became interested in NMR and studied structures and dynamics of nucleic acids. In the late 1970's, he spent a year and a half at the Max-Planck-Institut (Heidelberg) by Humboldt Research Fellowship when he began NMR studies of proteins. In 1992, he moved to Kobe University as a full professor, when he started high-pressure NMR to study protein dynamics in solution. He introduced the pressure-resisting cell system developed by his colleague to protein dynamic studies. Since then, his research has been strongly focused on exploring the dynamic aspect of protein structures using pressure perturbation, particularly with high-pressure NMR. In 1998, he received the Humboldt Award for his distinguished high-pressure NMR work, and since 1999, he has been an honorable member of the Indian Magnetic Resonance Society. He is now at Kinki University in Wakayama Prefecture, located south of Osaka and continues research activity with a lot of international collaboration using the high-pressure NMR facility at RIKEN Harima Institute, where he is a senior visiting scientist.

## 1. Introduction

Protein molecules, linear polymers of amino acids connected by peptide bonds, have through their  $\phi$  and  $\psi$  angles a freedom of rotation that endows their polypeptide chains with intrinsic conformational flexibility. The three-dimensional, folded structure of a native protein is determined by countless numbers of molecular interactions, a large number of which involve solvent water. The functional conformation of a protein is basically labile and dependent upon environmental parameters. As a consequence, a biologically active protein is a dynamic entity that can respond quickly to changes in the environment.

This motility is a key to protein function, and to understand the biological activity of proteins, their static structure given

\* To whom correspondence should be addressed. Telephone: 81-736-77-0345, ext. 4110. Fax: 81-736-77-4754. E-mail: akasaka8@spring8.or.jp.

by X-ray crystallographic coordinates must be augmented by the dynamic structure evident from biochemical and spectroscopic measurements in solution. Beside other techniques, circular dichroism (CD), fluorescence, Fourier transform infrared spectroscopy (FTIR), nuclear magnetic resonance (NMR) spectroscopy, and molecular dynamics calculation are favored by protein researchers to elucidate protein dynamics in solution, often with external perturbations or jump methods. Among these, NMR is unique in that it can give residue-specific or atomic-detailed information under favorable conditions where modern multidimensional techniques are applicable. NMR spin relaxation is employed frequently for assessing rapid fluctuations in protein structure. However, it is limited in applicable time range and usually lacks structural information associated with fluctuation.

Apart from rapid fluctuations of atoms anticipated in any molecules in solution, proteins are also endowed with slow conformational fluctuations involving concerted motions of some atoms. Slow fluctuations or rare events in protein conformational dynamics are much less studied but could be decisively important in protein function, because they are more likely to be evolutionally designed. In other words, the information is presumably encoded in the sequence of the DNA and therefore of the protein. Although evidence for slow fluctuations of proteins has been obtained in solution from experiments such as NMR-detected hydrogen exchange rate measurements, they do not directly give structural information on rare conformers, i.e., how the average structure is “deformed” in the fluctuation. To gain direct information on the conformational excursions associated with internal motions, one must amplify the fluctuations in such a way that the “deformed” structure is sufficiently populated to be detected by spectroscopic means. Temperature and chemical perturbations, including pH, ionic strength, denaturing agent, etc., are commonly employed for this purpose. Thermodynamic aspects of temperature perturbation to protein structures are well-established,<sup>1</sup> giving a basis for understanding how and why temperature affects global conformational equilibria of proteins. Chemical perturbations such as pH and denaturants are also used frequently. However, many fluctuation “deformations” separated by small energy differences will be too strongly affected by temperature or chemical perturbation and are likely to be overlooked.

Pressure is a fundamental thermodynamic variable for defining protein conformational states.<sup>2</sup> A protein in solution generally equilibrates among multiple conformational sub-states, differing in partial molar volume. Pressure affects conformational equilibria through volume differences, in contrast to temperature and chemical changes, which perturb conformational equilibria through heat capacity differences. Molar volume differences associated with conformation are relatively large for macromolecules, including proteins. Pressure provides a simple, clean, and efficient means of shifting the population distribution among fluctuating conformers of a protein and increasing the population of an otherwise rare conformer (by a few orders of magnitude in favorable cases). The conformer may then be amenable to spectroscopic observation and analysis within the relatively mild pressure range of a few kilobars.

The recognition of a strong effect of pressure on the protein conformation dates back to the early 20th century when Bridgman showed that egg albumen coagulates completely at pressures of 700 MPa.<sup>3</sup> Pressure denaturation of proteins

became a subject of interest, and the first  $P,T$  phase diagram on protein denaturation was presented by Keizo Suzuki in 1960,<sup>4</sup> followed by determination of more rigorous  $P-T$  diagrams in 1970s by various workers in the U.S.A. using UV difference spectroscopy, fluorescence, in 1980s, also vibrational spectroscopy, and, more recently, small angle X-ray scattering (SAXS) and NMR. In addition to thermodynamic interest, the use of pressure perturbation to study conformational dynamics in proteins has gradually increased during the past decades using site-specific probes such as Trp fluorescence,<sup>5</sup> NMR spectroscopy,<sup>6–10</sup> and FTIR spectroscopy.<sup>11</sup> Within the past decade, in particular, there has been a dramatic increase in the literature reporting high-pressure studies of proteins. This is due not only to advances in recombinant techniques for producing proteins and to increased interest in the dynamic aspects of the protein structure and function but also to the development of new techniques such as high-pressure NMR and molecular dynamics. Following the pioneering but limited range of works by Wagner and Morishima,<sup>6,7</sup> Jonas et al. extended the use of high-pressure NMR to a wider range of targets including protein denaturation, intermediate structures, and cold denaturation.<sup>12</sup> In recent years, interest has increased in using multidimensional NMR spectroscopy for pressure studies, because of its exceptionally high content in structural information.<sup>10,13</sup>

This review focuses on recent developments in protein dynamics using NMR spectroscopy along with pressure perturbation. The basic dynamic concept of proteins discussed here shares much with that by Frauenfelder et al.,<sup>11</sup> which is primarily based on experiments on myoglobin using absorption and FTIR spectroscopy, along with pressure and temperature perturbations. The recent development of high-resolution, multidimensional, variable-pressure NMR spectroscopy with pressure-resistive cell techniques,<sup>10,13</sup> however, has expanded the target proteins, the conformational space, and the frequency of motion to be studied by pressure perturbation to much wider ranges. Sections 2 and 3 are intended to acquaint the reader with the methodology. Sections 4–6 explore a broad range of applications of pressure perturbation, with specific examples rather than exhaustive iterations. For earlier reviews on protein structure and dynamics reported from high- or variable-pressure NMR studies, the reader is referred to Jonas<sup>14</sup> and Akasaka.<sup>15</sup>

For the pressure unit, either MPa or bar is used, whichever is convenient (1 bar =  $10^5$  Pa = 0.9869 atm).

## 2. Basic Rules Governing Pressure and Proteins

### 2.1. Response of a Protein to Pressure

The effective volume of a protein molecule in an aqueous environment (including the contribution from hydration) is represented by the partial specific or partial molar volume, because the volume of the protein and that of water is inseparable. A greatly simplified view of the fluctuation of a partial molar volume of a protein shown in Figure 1 may help understand qualitatively what is expected to happen to protein structures under pressure.<sup>16</sup> We may consider two categories of volume fluctuation for a protein system in solution: category (A), the fluctuation within a subensemble of the conformer (e.g., the folded conformer); and category (B), the fluctuation between different subensembles of conformers characterized with different free-energy levels. Under pressure, the partial molar volume of the protein

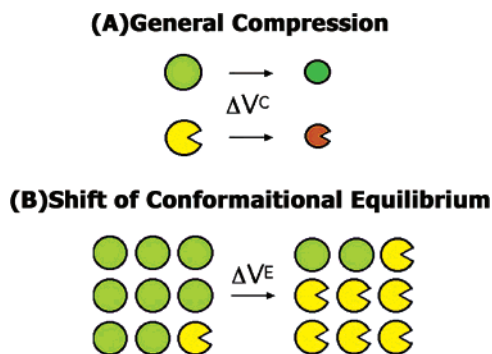


**Figure 1.** Schematic representation showing two categories of volume changes by pressure for a protein system in solution: category (A), the general compression within a subensemble of the conformer (e.g., the basic folded conformer N); and category (B), the shift of conformational equilibrium between different subensembles of conformers (N and I) characterized with different free-energy levels.

system may become smaller through the combination of these two categories of fluctuations, although in reality, clear distinction between the two cases may not always be possible. The categories A and B are close to those that Frauenfelder et al. discussed earlier as elastic and conformational pressure effects, respectively.<sup>11</sup>

## 2.2. General Compression within a Subensemble of Conformers

In a simple case where fluctuation takes place within a single subensemble, e.g., the basic folded subensemble N (Figure 1A), the mean-square fluctuation of the volume of a protein [ $\langle(\delta V)^2\rangle$ ] is intimately related to the isothermal compressibility ( $\beta_T V$ ) of the protein through the relation

$$\langle(\delta V)^2\rangle = \beta_T V k T \quad (1)$$

$$\beta_T = -(1/V)(\partial V/\partial p)_T$$

$$\beta_T = \beta_S + \alpha^2 T V / C_p \quad (2)$$

where  $V$  is the partial volume of the protein,  $\beta_T$  is the isothermal compressibility coefficient,  $\beta_S$  is the adiabatic compressibility coefficient,  $\alpha$  is the thermal expansivity,  $k$  is Boltzmann's constant, and  $T$  is the absolute temperature.<sup>17</sup> Equation 1 indicates that we acquire information on the amplitude of volume fluctuation from the value of the isothermal compressibility, i.e., compression per unit pressure under equilibrium condition. Microscopically, the compression of the partial volume is attained by a shift of the population among microscopic substates within the basic folded state in favor of microscopic substates having lower volumes.

Classically, adiabatic compressibility has been measured as macroscopic values for proteins in solution using ultrasonic velocity measurements, from which isothermal compressibility is calculated using eq 2 and then the volume fluctuation using eq 1.<sup>18</sup> For many globular proteins, root-mean-square (rms) fluctuations of the volume obtained in this way are on the order of  $\sim 0.3\%$  of the total volume  $V$ . One should note, however, that eq 1 should hold only approximately for proteins and that the rms fluctuations deduced should refer to those in a frequency of  $\sim$  megahertz or higher because of the ultrasonic frequency ( $\sim$  megahertz) used for measurements.

Nonetheless, macroscopic compressibility must have its origin in changes in average interatomic distances (microscopic compressibility). Crystallographic experiments at high pressure can give information on microscopic or site-specific compression of a protein molecule, with the first successful example being the application to hen lysozyme<sup>19</sup> and then to myoglobin.<sup>20</sup> It was revealed that compression is heterogeneous, involving local expansion. Thus far, the technical difficulty of getting stable crystals under pressure has hampered a wide application, although this situation is being rapidly improved. Measurement of microscopic compressibility has become an experimental feasibility also in solution since the introduction of high-resolution high-pressure NMR spectroscopy.<sup>21,22</sup> Compression of the secondary and tertiary structures is manifested in pressure-induced  $^1\text{H}$  chemical shifts of the amide and side-chain protons,<sup>22</sup> which are converted to interproton distance changes,<sup>23–25</sup> or in pressure-induced changes in  $^1\text{H}$  NOE,<sup>26</sup> directly giving changes in interproton distances. Again, the results give heterogeneous compression involving local expansion. Because NMR measurement takes time (minutes, hours, or days), pressure-induced shifts should in practice include contributions from all slow equilibrium responses of the protein structure.

## 2.3. Shift of Equilibrium between Different Subensembles of Conformers

In general, a protein molecule in solution may exist as an equilibrium mixture of subensembles of conformers differing, in general, in folding topology (e.g., between the native subensemble N and an intermediately folded subensemble (designated by I, cf. Figure 1B), in thermodynamic stability ( $\Delta G = G_I - G_N$ ) as well as in partial molar volume ( $\Delta V = V_I - V_N$ ). In this situation, the equilibrium constant  $K$  between conformers N and I may change with pressure according to the relation

$$K = [I]/[N] = \exp(-\Delta G/RT) \quad (3)$$

$$\Delta G = G_I - G_N = \Delta G(p_0) + \Delta V^\circ(p - p_0) - (1/2)\Delta\beta V^\circ(p - p_0)^2 \quad (4)$$

Here,  $\Delta G$  and  $\Delta G(p_0)$  are the Gibbs energy changes from N to I at pressure  $p$  and  $p_0$  (1 bar), respectively;  $\Delta V^\circ$  is the partial molar volume change at  $p_0$  (1 bar);  $\Delta\beta$  is the change in compressibility coefficient;  $R$  is the gas constant; and  $T$

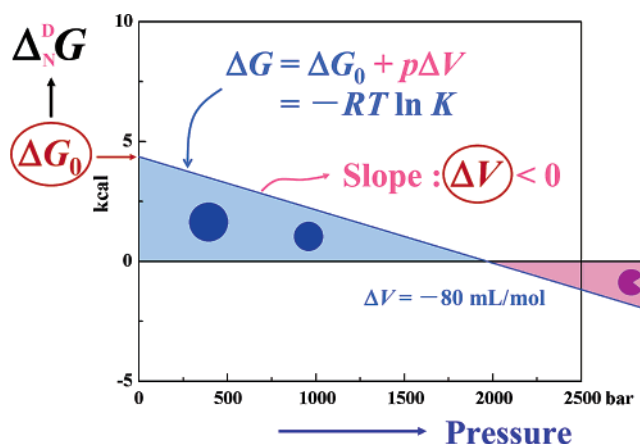


**Figure 2.** Schematic expression of eq 4 by neglecting the second-order term. A specific case with  $\Delta V = -80$  mL/mol and  $\Delta G^\circ = \sim 4$  kcal/mol is drawn.

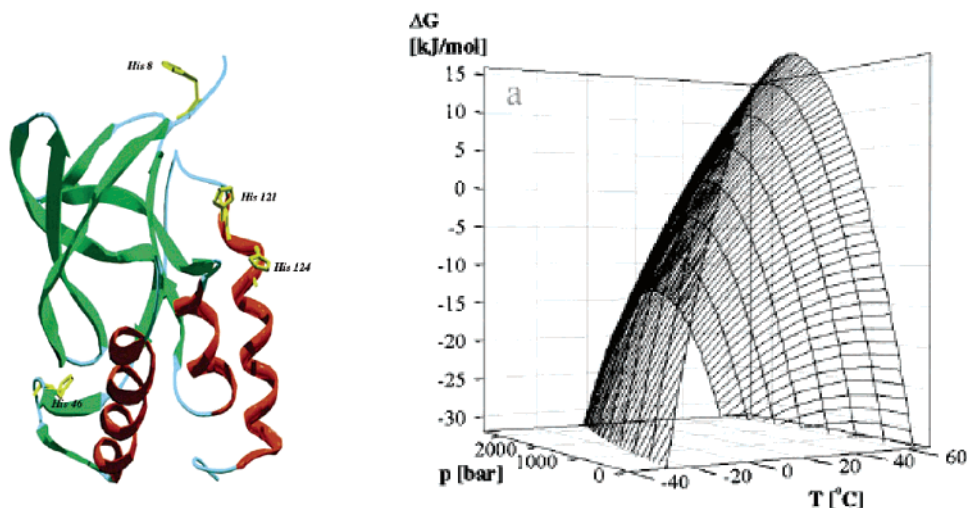


**Figure 3.** Stability of *Staphylococcal* nuclease against the temperature and pressure. Parameters determined by fitting NMR data to eq 5 are  $t_c$  (°C) =  $-8.1 (\pm 0.4)$ ,  $t_h$  (°C) =  $42.7 (\pm 2.1)$ ,  $\Delta C_p$  [kJ/(mol K)] =  $13.12 (\pm 2)$ ,  $\Delta S^\circ$  [kJ/(mol K)] (at 51.2 °C) =  $1.51 (\pm 0.23)$ ,  $\Delta V^\circ$  (mL/mol) (at 1 bar and 24 °C) =  $-41.9 (\pm 6.3)$ ,  $\Delta\alpha$  [mL/(mol K)] =  $1.33 (\pm 0.2)$ ,  $\Delta\beta$  [mL/(mol bar)] =  $0.02 (\pm 0.003)$ . Reprinted with permission from ref 32. Copyright 2000 Elsevier, The Netherlands.

is the absolute temperature. Often, the third term of eq 4,  $-1/2\Delta\beta V^\circ(p - p_0)^2$ , is not significant below  $\sim 2$  kbar, resulting in an approximately linear dependence of  $\Delta G$  on  $p$  with a slope  $\Delta V$  closely represented by  $\Delta V^\circ$  (Figure 2). Under physiological conditions,  $\Delta G^\circ$  is normally positive (i.e., N is more stable than I), and then the population of conformer I is too low to be detected. Even if  $\Delta G^\circ$  is as small as  $\sim 1$ – $2$  kcal/mol, the equilibrium population of I is on the order of  $\sim 10\%$ , making the NMR detection of conformer I quite difficult. *Molecular interaction depends upon energy, while spectroscopic detection depends upon population.* Here, pressure works its magic. For a typical  $\Delta V^\circ$  value from  $-20$  to  $-100$  mL/mol for a globular protein,<sup>27</sup> the  $\Delta V^\circ(p - p_0)$  term amounts to  $-1$  to  $-5$  kcal/mol at 2 kbar, sufficiently large to compensate a marginal  $\Delta G^\circ$  (a few kcal/mol) and to change the sign of  $\Delta G$  (Figure 2). *The population enhancement of the rare conformer I by a few orders of magnitude may be attained.* When I is stably trapped as a major conformer under pressure, the NMR measurement may be done continuously for hours or even days.

When both temperature and pressure are varied

$$\Delta G = G_I - G_N = \Delta G^\circ - \Delta S^\circ(T - T_0) - \Delta C_p[T\{\ln(T/T_0) - 1\} + T_0] + \Delta V^\circ(p - p_0) - (1/2)\Delta\beta V^\circ(p - p_0)^2 + \Delta\alpha(p - p_0)(T - T_0) \quad (5)$$

or by using Taylor expansion

$$\Delta G = G_I - G_N = \Delta G^\circ - \Delta S^\circ(T - T_0) - (1/2)(\Delta C_p/T_0)(T - T_0)^2 + \Delta V^\circ(p - p_0) - (1/2)\Delta\beta V^\circ(p - p_0)^2 + \Delta\alpha(p - p_0)(T - T_0) \quad (6)$$

must be used. In the temperature range under investigation, the heat capacity ( $\Delta C_p$ ), thermal expansion coefficient ( $\Delta\alpha$ ), and isothermal compressibility change ( $\Delta\beta$ ) are assumed to be constant and independent of the temperature and pressure, although recent results using pressure perturbation calorimetry depict a significant temperature dependence of the  $\Delta\alpha$  value. Equation 6 gives an ellipsoid (or more correctly half-ellipsoid like that in Figure 3, left, for *Staphylococcal* nuclease<sup>32</sup>). It is to be noted that at physiological or lower

temperatures  $\Delta G$  is normally a single-valued function of pressure, whereas at constant pressure,  $\Delta G$  is a double-valued function of temperature with transitions at  $t_h$  (heat denaturation) and  $t_c$  (cold denaturation). The  $P$ – $T$  phase diagram gives the basis for understanding thermodynamic stability of globular proteins on the  $P$ – $T$  plane, but the reader should note that eqs 5 and 6 apply only to the case of a two-state transition. While a strict two-state transition is rare for a globular protein, the equations may generally apply to a transition between any two distinct states of a protein.

In the early 1970s, Brandts,<sup>28</sup> Hawley,<sup>29</sup> and Kauzmann<sup>30</sup> explored the temperature–pressure phase behavior of ribonuclease A, chymotrypsinogen, and metmyoglobin unfolding, respectively, by optical absorption, and more recently, Royer and Winter<sup>31</sup> by fluorescence, FTIR, and SAXS and Lassalle et al.<sup>32</sup> by proton NMR studied the stability of *Staphylococcal* nuclease on  $P$ – $T$  axes and determined thermodynamic parameters in eq 5 or 6.

### 3. Experimental Techniques To Explore Pressure Effects on Proteins

#### 3.1. Established Techniques for General Compression and Global Conformational Changes

Methods used to monitor the fluctuation in category A are rather limited. Most information has been obtained from ultrasonic velocity measurement.<sup>18,33</sup> Although there are only two crystal structures at high pressure,<sup>19,20</sup> they give important site-specific information on conformational fluctuation through eq 1. High-pressure NMR using two-dimensional spectroscopy also gives microscopic compressibility information. This subject will be described in more detail later.

A global change of conformation with pressure can be studied with a number of different techniques, including high-pressure fluorescence<sup>34,35</sup> and FTIR<sup>36,37</sup> and, more recently, with SAXS.<sup>38,39</sup> One-dimensional <sup>1</sup>H NMR spectroscopy can also be used for quantitative evaluation of conformational equilibrium as a function of the pressure combined with qualitative information about the structures of the conformers as already described. CD measurements at high pressure have been hampered because of the effect of distortion of windows

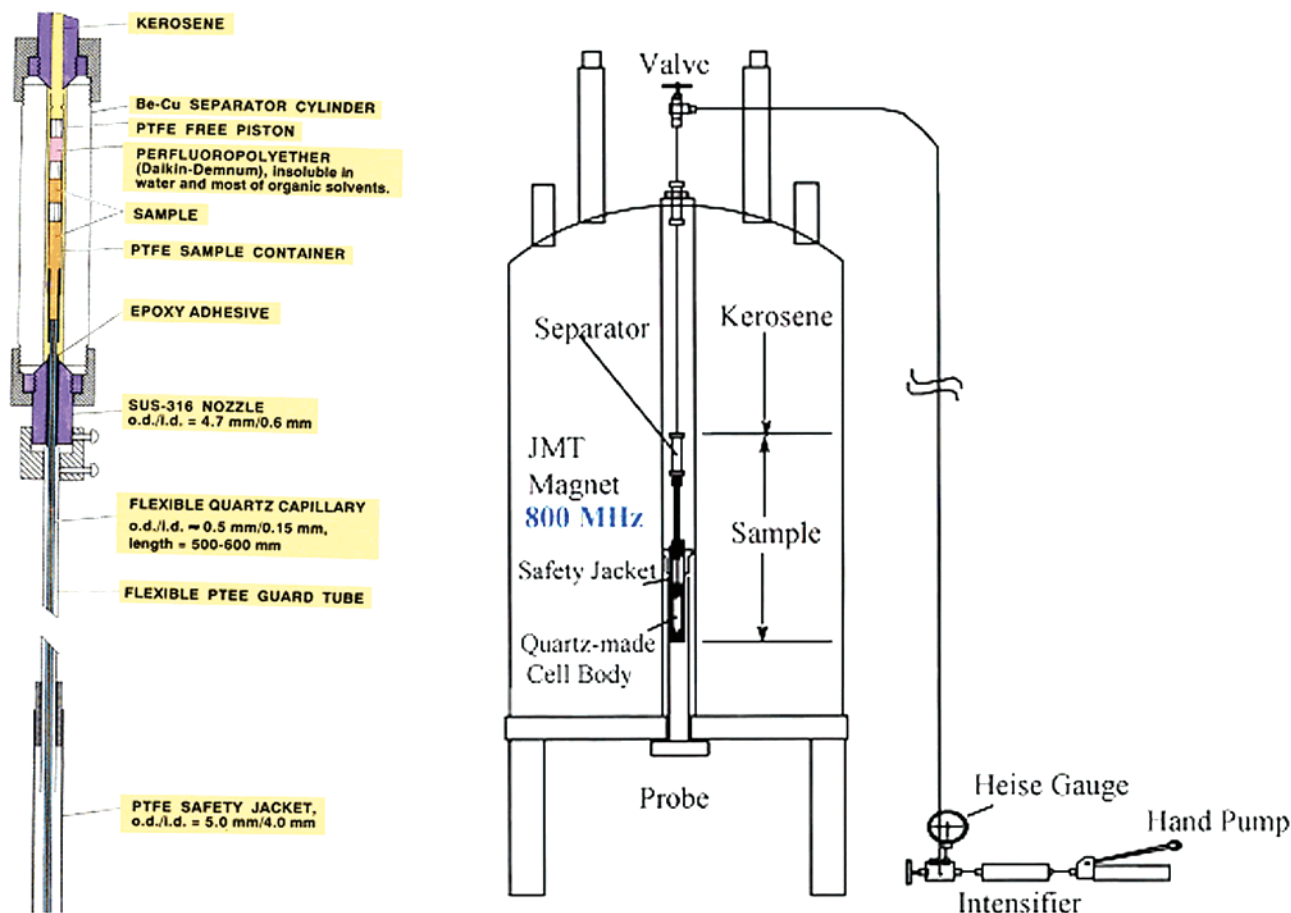


**Figure 4.** One-line cell high-pressure NMR system with a pressure-resisting quartz cell. See ref 43 for more details.

under pressure. Except for X-ray scattering and high-pressure NMR using pressure-resistive cells, pressures are the same in the inside and outside of the sample cell so that very high pressure in the range of 400–1000 MPa can be applied. It is to be emphasized that, to determine thermodynamic parameters in eqs 4–6 using the above techniques, the system must behave in a two-state manner. Most proteins, however, do not behave strictly two-state under pressure.

### 3.2. High-Pressure NMR Technique for Site-Specific Conformational Changes

Measurements using intrinsic Trp fluorescence report specifically environmental changes of Trp residues and could be site-specific for a protein with only one Trp. (see Royer on this issue). In general, however, in a multitryptophan protein, it is difficult to assign observed changes in fluorescence to global versus local changes of conformation or to local environmental changes of specific Trp residues. With limited success, one can also use one-dimensional  $^1\text{H}$  NMR spectroscopy to study site-specific changes of conformation with pressure, for example, by monitoring Trp side-chain signals, which often appear as mutually separate peaks in the lowest field part of the spectrum. Special lines of absorption in infrared spectroscopy can also be used to report specific conformational states and conformational dynamics in selected proteins.<sup>40</sup>

Site-specific fluctuations and changes in conformation can be more generally studied with two- or multidimensional NMR spectroscopy combined with pressure. Hydrogen/deuterium exchange for amide protons is carried out at high

pressure off line, and the two-dimensional NMR measurements can be carried out after bringing the pressure back to 1 bar to determine the site and degree of hydrogen/deuterium exchange reactions proceeded. However, our limited understanding of the mechanism of pressure effect on hydrogen exchange rate precludes its use as a general method for conformational fluctuation.<sup>41</sup>

High-pressure NMR (or variable-pressure NMR) has become a major source of information in delineating site-specific details of pressure effects on protein structures.<sup>14,15</sup> Technically, two different approaches have been taken: one pressurizing the entire NMR probe in an autoclave and the other pressurizing the sample cell, only leaving the probe itself at 1 bar. The former has the advantage of a larger sample volume and high working pressure even up to  $\sim 900$  MPa but has thus far failed to attain sufficiently high magnetic field homogeneity and versatility in the pulse sequence necessary to perform heteronuclear two- or multidimensional measurements at high resolution. The latter approach has the disadvantage of a smaller sample volume and limited working pressure ( $< 3$  kbar in the quartz cell design) but has a sufficiently high resolution for performing heteronuclear two- or multidimensional measurements with versatile pulse sequences. By now, pressurizing the sample cell has proven to be the method of choice for protein NMR studies under pressure. Various materials have been tested for the cell, including glass, sapphire,<sup>42,44</sup> and quartz.<sup>43</sup> Thus far, the handmade quartz cell has been most successful.<sup>43</sup> A detailed description of the design of the quartz cell and its handling is found in ref 40, the typical experimental procedure with which is the following.

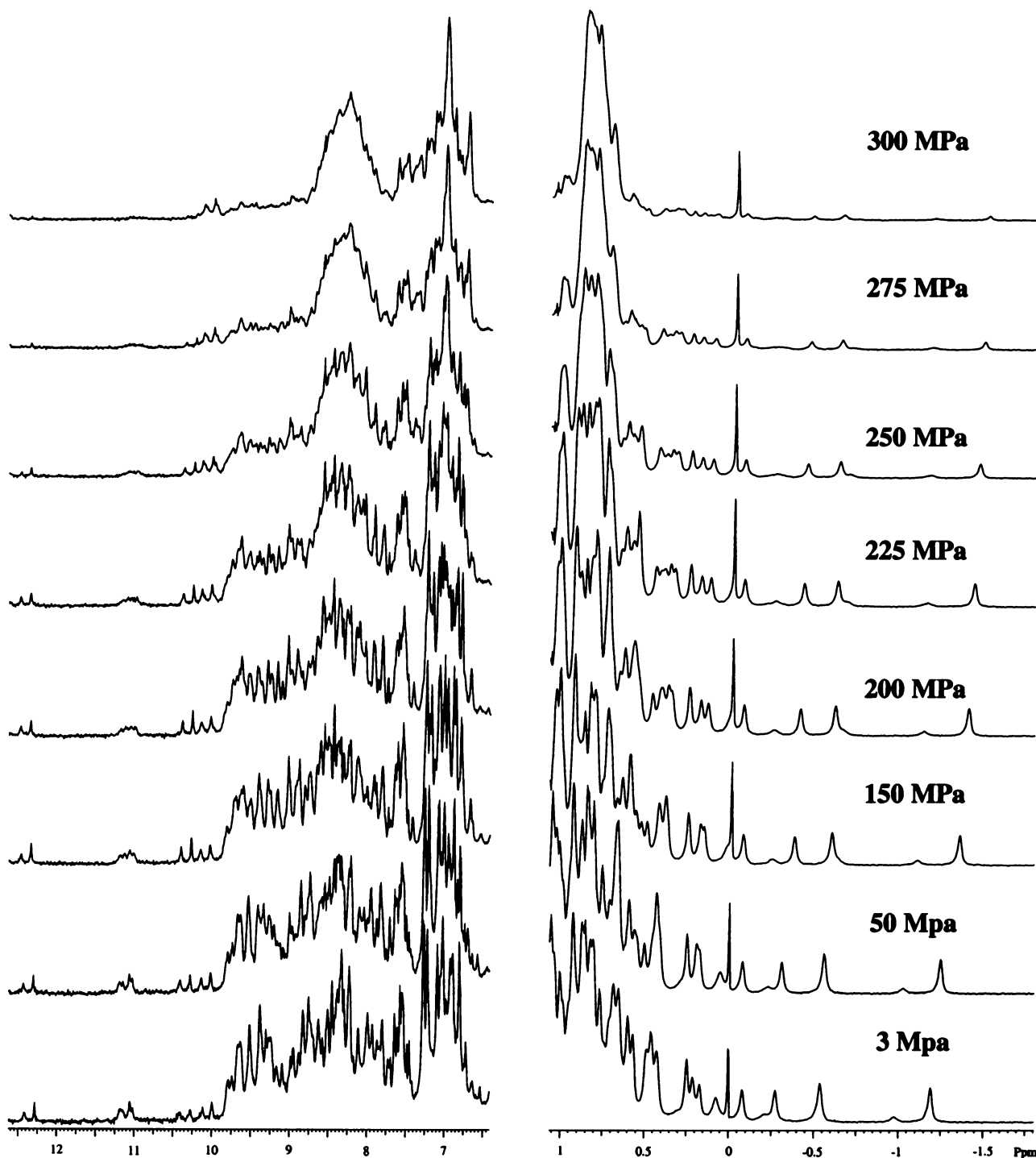


**Figure 5.** Example showing the effect of pressure on the one-dimensional  $^1\text{H}$  NMR spectrum of a globular protein ( $\text{P13}^{\text{MTCPI}}$ ). Each spectrum results from the co-addition of 2000 transients. Spectra were measured at a protein concentration of 1 mM in 10 mM Tris buffer at pH 7.0 and 20 °C. Several methyl proton signals at the high-field side ( $>0$  ppm) at 3 MPa are identified as Leu103  $\text{C}\delta\text{H}_3$  ( $-0.08$  ppm), Leu13  $\text{C}\delta\text{H}_3$  ( $-0.27$  ppm), Leu13  $\text{C}\delta\text{H}_3$  ( $-0.54$  ppm), and Leu101  $\text{C}\delta\text{H}_3$  ( $-1.19$  ppm). The tryptophan side-chain signals are at the extreme low-field edge of the spectrum. The shift of these methyl signals further to the high field with increasing pressure shows the compression of the core part of the folded protein (general compression), whereas their intensity decrease with pressure shows that some fraction of the folded protein undergoes unfolding (shift of equilibrium) with increasing pressure. Both effects are clearly distinguished but take place simultaneously. The spectral change (both the shift and the intensity change) is fully reversible with pressure. Reprinted with permission from ref 70. Copyright 2002 Elsevier, The Netherlands.

The protein solution is contained in a quartz tube, the body part of which, consisting of an inner diameter less than 1 mm and an outer diameter of  $\sim 3$  mm protected by a Teflon jacket, is inserted into a commercial NMR probe of a 5 mm sample tube (Figure 4). The protein solution is separated from the pressure mediator (kerosene) by a frictionless piston made of Teflon in a separator cylinder made of BeCu. The pressure

is adjusted with a remotely located hand pump to a desired value between 1 and  $\sim 3000$  bar (measured with a Heise Bourdon gauge) and is transmitted through a stainless steel tube containing kerosene to the sample solution in the quartz tube. An excellent spectral resolution is normally attained, practically limited by intrinsic line widths. Figure 5 gives an example of one-dimensional  $^1\text{H}$  NMR spectra for a

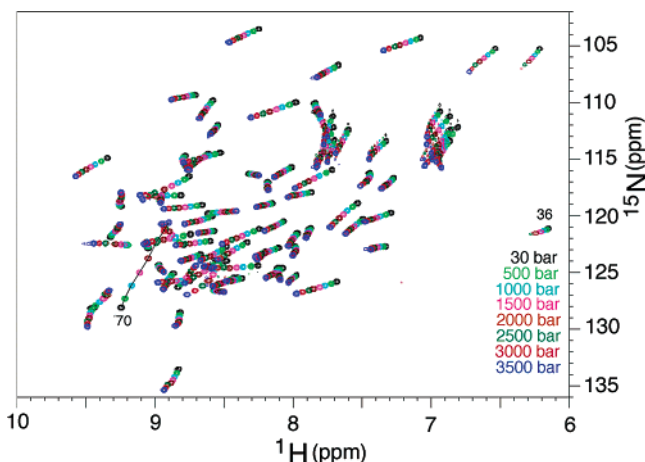


**Figure 6.** Example showing the effect of pressure on the two-dimensional NMR spectrum of a protein ( $^{15}\text{N}$ -uniformly labeled ubiquitin). Superimposed  $^{15}\text{N}/^1\text{H}$  HSQC spectra from 30 to 3500 bar at 20 °C (black, 30 bar; light green, 500 bar; blue, 1000 bar; pink, 1500 bar; brown, 2000 bar; green, 2500 bar; red, 3000 bar; and purple, 3500 bar). Spectra were measured at a protein concentration of 2.0 mM in 30 mM acetate buffer (95%  $^1\text{H}_2\text{O}/5\%$   $^2\text{H}_2\text{O}$  at pH 4.5). The spectral change is fully reversible with pressure.

globular protein P13<sup>MTCPI</sup> at various pressures up to 3000 bar, and Figure 6 gives an example of two-dimensional  $^{15}\text{N}/^1\text{H}$  heteronuclear single-quantum correlation spectroscopy (HSQC) for  $^{15}\text{N}$ -uniformly labeled ubiquitin at various pressures up to 3500 bar.

#### 4. Probing Fluctuations within the Folded Subensemble of Conformers

The use of pressure-coupled NMR experiments to probe the folded ensemble of proteins has been pioneered with one-dimensional proton NMR by Wagner and Morishima.<sup>6,7</sup> The recently developed NMR techniques to monitor pressure

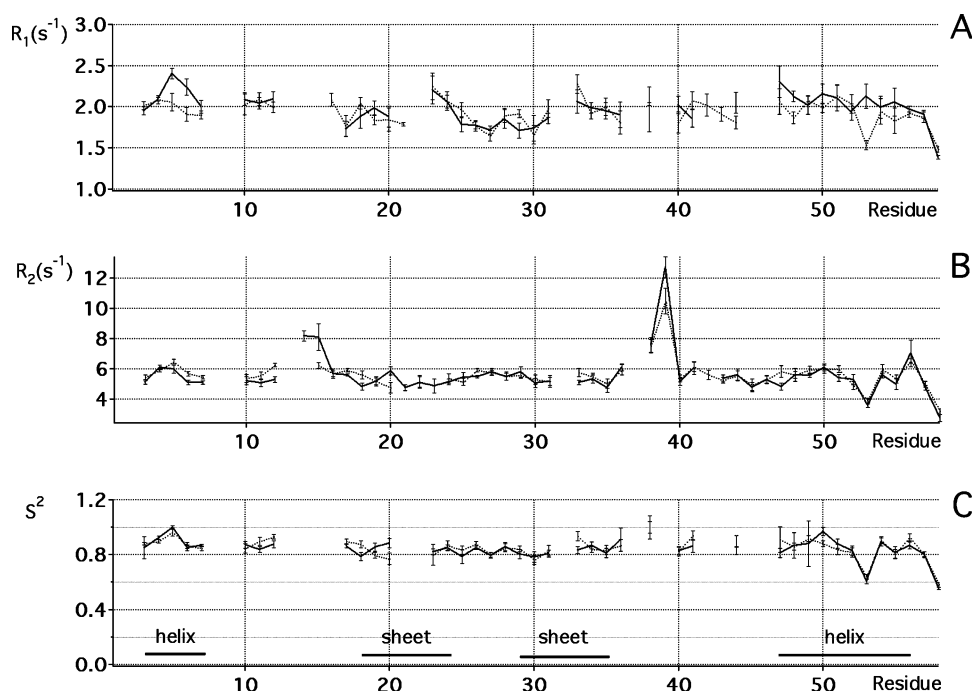
effects on the protein structure at kilobar ranges using two- or multidimensional NMR spectroscopy<sup>21,22,41,45</sup> have revolutionized the study of pressure effects on protein structure and dynamics to the full versatility of modern heteronuclear NMR spectroscopy.

#### 4.1. Backbone Dynamics from Spin Relaxation

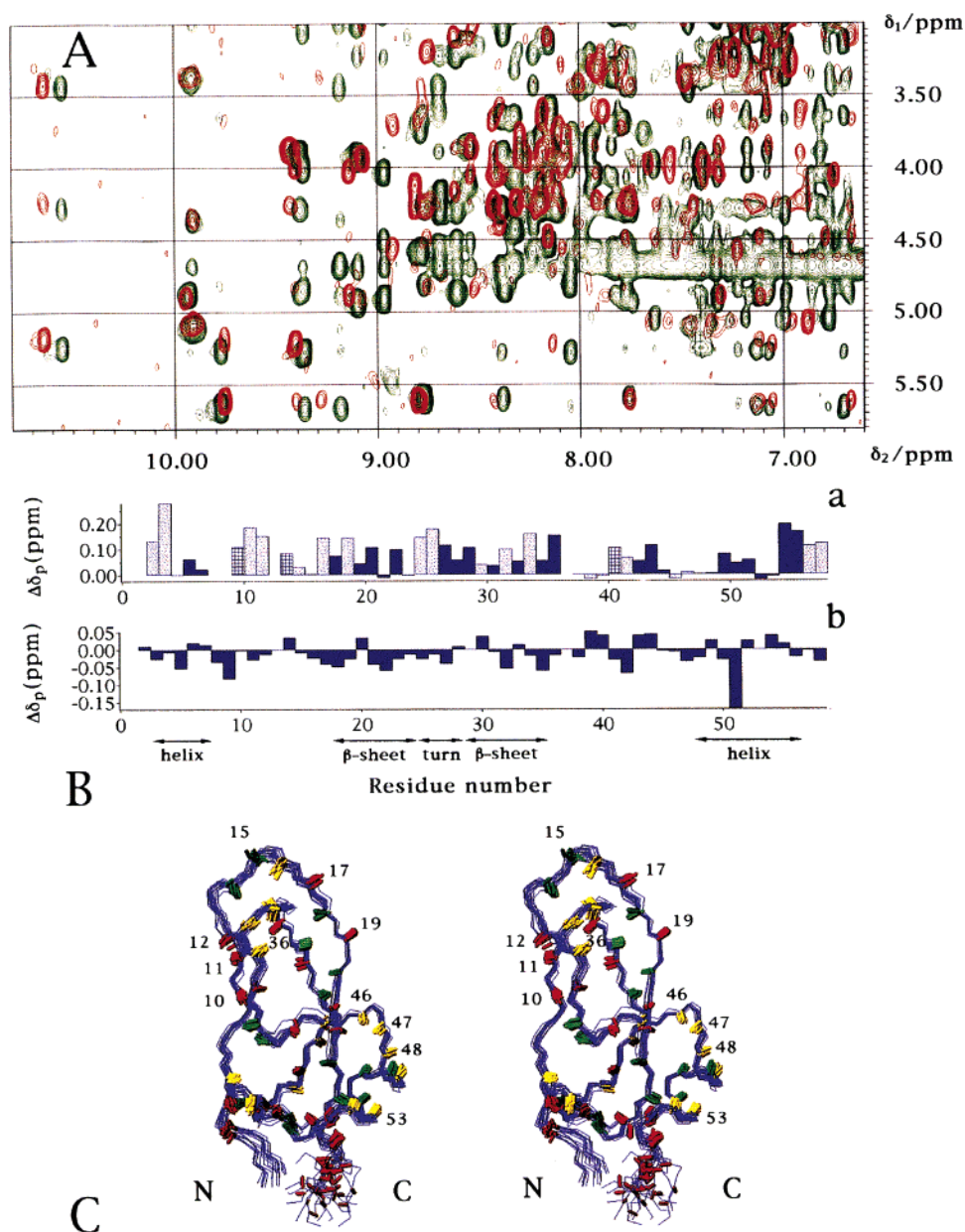
$^{15}\text{N}$  spin relaxation analysis on a  $^{15}\text{N}$ -uniformly labeled protein is a frequently used technique to probe rapid (pico–nanosecond) internal dynamics of a polypeptide backbone.<sup>46</sup> Because protein dynamics is generally sensitive to pressure, there arises naturally a question if  $^{15}\text{N}$  spin relaxation may be useful to examine the effect of pressure on protein dynamics. A few proteins<sup>47–50</sup> have thus far been studied with this technique to probe effects of pressure on spin relaxation dynamics.

Figure 7 shows the superposition of  $^{15}\text{N}$  relaxation rates ( $R_1$  and  $R_2$ ) measured at 30 bar and 2 kbar for 41 protonated backbone  $^{15}\text{NH}$  of  $^{15}\text{N}$ -uniformly labeled bovine pancreatic trypsin inhibitor (BPTI) in aqueous solution at pH 4.6 and 36 °C.<sup>47</sup> BPTI remains fully folded at 2 kbar, and the viscosity of water also remains similar between 30 bar and 2 kbar. Figure 7C shows that under this condition the Lipari and Szabo order parameters<sup>46</sup> remain unchanged in the range of 0.8–1 at both pressures. This indicates that rapid internal motions of individual NH vectors ( $\ll$ nanoseconds) are not altered at all by pressure at 2 kbar. Similar results were obtained for an isolated  $\alpha$  helix from bacteriorhodopsin in an organic solvent, although at 2 kbar, the overall rotational diffusion of the molecule slows down by 3-fold because of the increase of viscosity.<sup>48</sup> The result simply means that the rapid internal motions ( $\ll$ nanoseconds) of NH vectors exhibit no significant activation volumes.

If the compressibility also depends upon similar rapid motions, the lack of change in the amplitude of fluctuation as represented by the order parameters, through eq 1, would predict that compressibility coefficients  $\beta$  should also be



**Figure 7.** Effect of pressure on rapid (nano–picosecond) dynamics of  $^{15}\text{N}$ -uniformly labeled BPTI at a proton frequency of 750.13 MHz at 36 °C and pH 4.6. A, B, and C represent  $^{15}\text{N}$  longitudinal ( $R_1$ ) and transverse ( $R_2$ ) relaxation rates and order parameter ( $S_2$ ) for individual amide groups, respectively, at 30 bar (—) and 2 kbar (⋯).<sup>47</sup>



**Figure 8.** Effect of pressure on hydrogen bonds of BPTI.<sup>22</sup> (A) Fingerprint (NH $\cdots$ C $_{\alpha}$ H) regions of the NOESY spectra of BPTI at 1 bar (green) and 2000 bar (red), measured at 750 MHz at 36 °C. The sample of BPTI was dissolved to a concentration of 10 mM in 200 mM acetate- $d_3$  buffer in 90%  $^1\text{H}_2\text{O}/10\%$   $^2\text{H}_2\text{O}$  at pH 4.6. (B) Histograms of pressure-induced  $^1\text{H}$  chemical shifts for individual peptide NH (a) and  $C_{\alpha}$  (b) at 36 °C. (C) Cross-eyed stereoview of the backbone atoms with positions and directions of the NH bonds, derived from 20 NMR structures and drawn using MOLMOL. The NH bonds with the largest pressure shifts are in red; medium shifts are in yellow; and very small shifts are in green. For more details, see ref 22.

constant with the pressure at all sites. As we shall see below, this prediction is supported by the linear pressure dependence of amide  $^1\text{H}$  and  $^{15}\text{N}$  chemical shifts with pressure for BPTI and the bacteriorhodopsin helix.

Rapid internal dynamics ( $\ll$ nanoseconds) do not vary by pressure in globular proteins such as hamster prion<sup>49</sup> and ubiquitin,<sup>50</sup> either. However, the slow dynamics ( $\gg$ nanoseconds) are affected by pressure, showing that they involve transition states with nonzero activation volumes.

## 4.2. Fluctuation from Pressure-Induced Shifts

### 4.2.1. Fluctuation in Hydrogen Bonds

Macroscopically, the isothermal compressibility coefficient  $\beta_T$  of a protein is related to the volume fluctuation through

eq 1,<sup>17</sup> which predicts that a protein with a larger compressibility is associated with a larger volume fluctuation. In principle, macroscopic compressibility is expected to be expressed in terms of microscopic compressibility, i.e., atom–atom distance changes per unit pressure, which may be manifested in chemical-shift changes. Despite the fact that spin relaxation shows minimal pressure-dependent changes of rapid internal dynamics on pressure, chemical shifts are quite sensitive to pressure<sup>22</sup> (Figure 8). The low-field shifts of amide  $^{15}\text{N}$  and  $^1\text{H}$  signals are attributable to the shortening of N–H bond distances with increasing pressure, and the available information indicates that the NH proton shift of a few hertz at the  $^1\text{H}$  resonance frequency of 750 MHz corresponds to an average linear compression of the hydrogen bond by as little as 0.001 Å.<sup>22</sup>



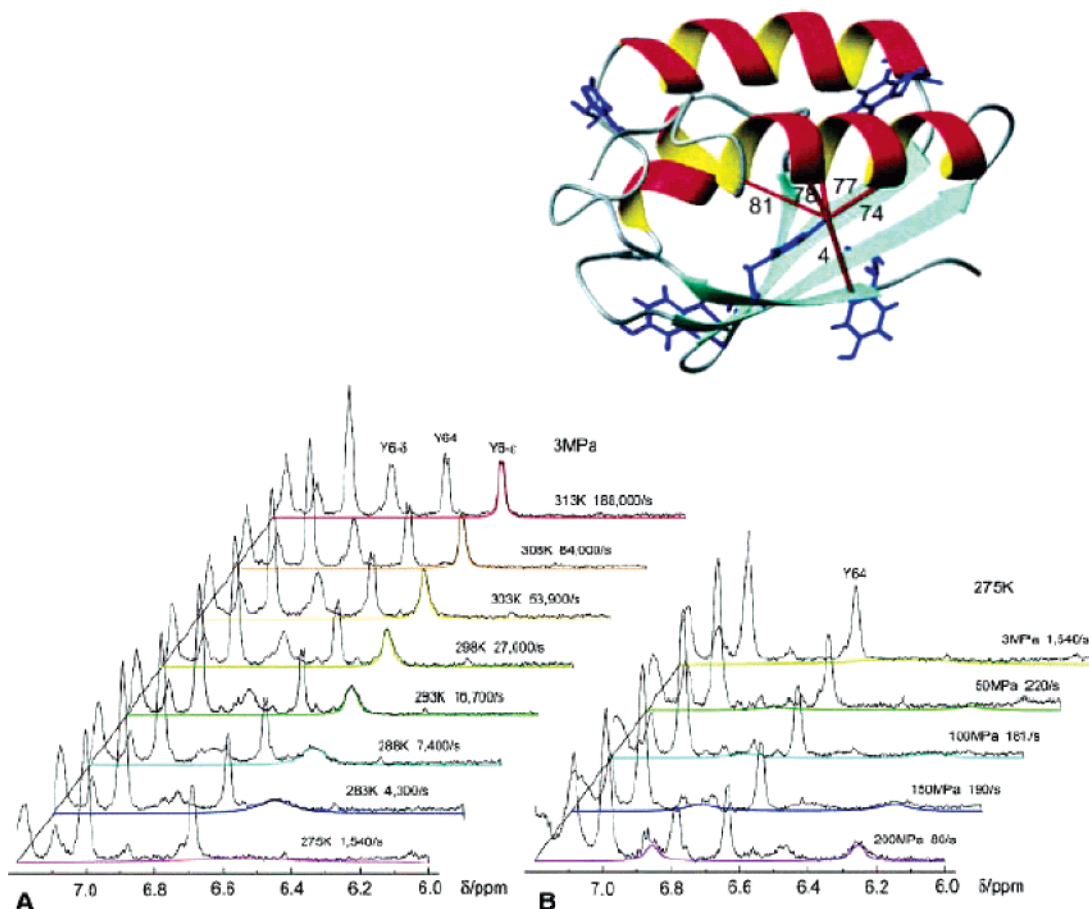


**Figure 9.** (Bottom) Experimental (black) and simulated (colored) ring proton signals of Tyr6. Line shapes of the  $H_{\epsilon 1, \epsilon 2}$  resonance(s) of Tyr6 were fitted with WinDNMR (A) at various temperatures at a constant pressure (30 bar) and (B) at various pressures at a constant temperature (275 K). (Top) Structure of HPr from *S. carnosus*. All of the aromatic rings are shown, with NOE contacts of the hydroxyl proton of Tyr6. See ref 58 for more details.

Surprisingly, the shifts are remarkably linear for all of the amide protons of BPTI, indicating pressure-independent compressibility at individual amide sites. This means from eq 1 that the amplitude of volume fluctuation remains the same for BPTI at 2 kbar as at 1 bar. The observed low-field shifts correspond to a shortening of N–H distances by 0.1 Å or 1% averaged over all of the  $NH \cdots O$  hydrogen bonds at 2 kbar.<sup>22</sup> The linear pressure dependence is not necessarily typical for globular proteins, as we shall see later. On the other hand, the pressure-induced shifts are quite heterogeneous over the molecule in Figure 8, indicating heterogeneous compressibility of the individual hydrogen bonds. For example, it predicts that the fluctuation is larger in the turn region and in the peripheral regions of the  $\beta$  sheet and the helix than in the interior parts of the  $\beta$  sheet and the helix.<sup>22</sup>

$^{15}N$  and  $^{13}C$  chemical shifts are more sensitive to pressure than those of the  $^1H$  in terms of relative shifts expressed in parts per million. The  $^{15}N$  pressure shift of the amide group is expected to provide additional information, namely, the fluctuation of torsion angles of the polypeptide backbone, although the information is qualitative.<sup>51</sup> An interesting application of  $^{15}N$  pressure shifts is that reported for  $^{15}N$ -labeled hen lysozyme, which showed abnormally large pressure shifts for amide groups in regions surrounding internal water molecules.<sup>52</sup> This qualitatively indicates that conformational fluctuation of the backbone is exceptionally large in the vicinity of internal water molecules, suggesting

that buried water molecules are the sites of preferred internal motions of a globular protein.

#### 4.2.2. Fluctuation in Tertiary Structure

Pressure-induced shifts of side-chain protons are sensitive probes for the general compression of the tertiary structure of a globular protein.<sup>21</sup> Williamson et al. developed a method to calculate changes of coordinates under pressure based on experimental  $^1H$  pressure-induced shifts of amide and side-chain protons and successfully applied it to hen lysozyme<sup>24</sup> and BPTI.<sup>25</sup> The changes of coordinates, although subtle, represent microscopic structural and volume fluctuations of these proteins taking place within the folded states of these proteins. The results indicate that the compression is quite heterogeneous over the folded molecule. In lysozyme at 2 kbar, the  $\alpha$  domain is compressed but the  $\beta$  domain is not, in perfect agreement with the crystallographic study reported earlier.<sup>19</sup>

Interestingly, the result arising from examining the locations of residues that have the largest changes in volume shows that they occur close to the buried water molecules, as predicted from  $^{15}N$  pressure shifts.<sup>52</sup> The volume changes are both positive and negative depending upon the location, demonstrating the heterogeneous fluctuation of the tertiary structure.<sup>24,25</sup> One of the most important implications from the above results is that the buried water molecules are preferred sites of conformational fluctuations in a folded globular protein.

### 4.2.3. Time Range of Fluctuations Sensed by Pressure-Induced Shifts

The range of frequency involved in the volume fluctuation is also a question of interest. The time range of pressure-dependent fluctuations can be slow, as long as seconds or even minutes, because the shift measurements are done in minutes and hours. However, NMR signals for folded BPTI showed sharp homogeneous Lorentzian lines at all pressures investigated, as if all of the interatomic distances were fixed. This is not true. The sharp lines only mean that any chemical-shift dispersion corresponding to intrateratomic distance distributions are time-averaged nearly completely by conformational fluctuations. How rapid can the fluctuations be? The lower limit of the fluctuation rates is the minimum frequency required to average out chemical-shift dispersion; for example, if the chemical-shift dispersion is  $\sim 0.05$ – $1$  ppm, fluctuations should occur well within micro-milliseconds for the sharp peak to be observed.

### 4.3. Infrequent Fluctuation of the Core Revealed from Ring-Flip Motions

There are cases, however, that fluctuations are much more infrequent than described above. The presence of infrequent ( $\sim 10^1$ – $10^6$  s $^{-1}$ ) fluctuations was demonstrated within the core of a globular protein first by one-dimensional NMR by Wagner in BPTI<sup>6,53–55</sup> and later by two-dimensional NMR by Li et al.<sup>26</sup> Slow ring flips of Tyr and Phe residues are present, and they are significantly retarded by pressure. Generally, slowly flipping ring systems are seldom observed in proteins because the flip must be hindered considerably by the atoms located above and below the ring plane. Since the first discovery in 1976 up to present, only a few examples of slow ring flips have been described in the literature and analyzed in details, including BPTI, cytochrome *c*,<sup>56,57</sup> and HPr.<sup>58</sup>

HPr from *Staphylococcus carnosus* is an 88-residue phosphocarrier protein with no disulfide bonds. One tyrosine (Tyr6) undergoes a very slow ring flip, the pressure and temperature dependence of which was studied in detail using the on-line cell high-pressure NMR technique over a pressure range from 3 to 200 MPa and a temperature range from 257 to 313 K (Figure 9).<sup>58</sup> The ring of Tyr6 is buried, sandwiched between a  $\beta$  sheet and  $\alpha$  helices (the water-accessible area is less than 0.26 nm<sup>2</sup>), with its hydroxyl proton being involved in an internal hydrogen bond with several surrounding residues. The ring flip rates on the order of  $\sim 10^1$ – $10^5$  s $^{-1}$  were determined from the NMR line-shape analysis of H $\delta$ 1, $\delta$ 2 and H $\epsilon$ 1, $\epsilon$ 2 of Tyr6, giving an activation volume  $\Delta V^\ddagger$  of  $0.044 \pm 0.008$  nm<sup>3</sup> ( $27 \pm 3$  mL mol $^{-1}$ ), an activation enthalpy  $\Delta H^\ddagger$  of  $89 \pm 10$  kJ mol $^{-1}$ , and an activation entropy  $\Delta S^\ddagger$  of  $16 \pm 2$  J K $^{-1}$  mol $^{-1}$ . The  $\Delta V^\ddagger$  value found for HPr ( $27 \pm 3$  mL/mol) falls within the relatively small range of 28–51 mL/mol found for the aromatic residues of BPTI. This observation fits well with the notion that the flip requires a minimum common space or cavity to be created around the ring. This extra space must be created as a result of cooperative thermal fluctuations of atoms surrounding the ring, occurring infrequently ( $10^3$ – $10^5$  s $^{-1}$ ) at ambient pressure. This model appears to be consistent with the dynamic nature of cavity formation<sup>59</sup> or a long-cherished mobile defect model such that water occasionally penetrates into the core of the protein,<sup>60,61</sup> used to interpret the phenomena of hydrogen exchange of an internal amide group with the bulk

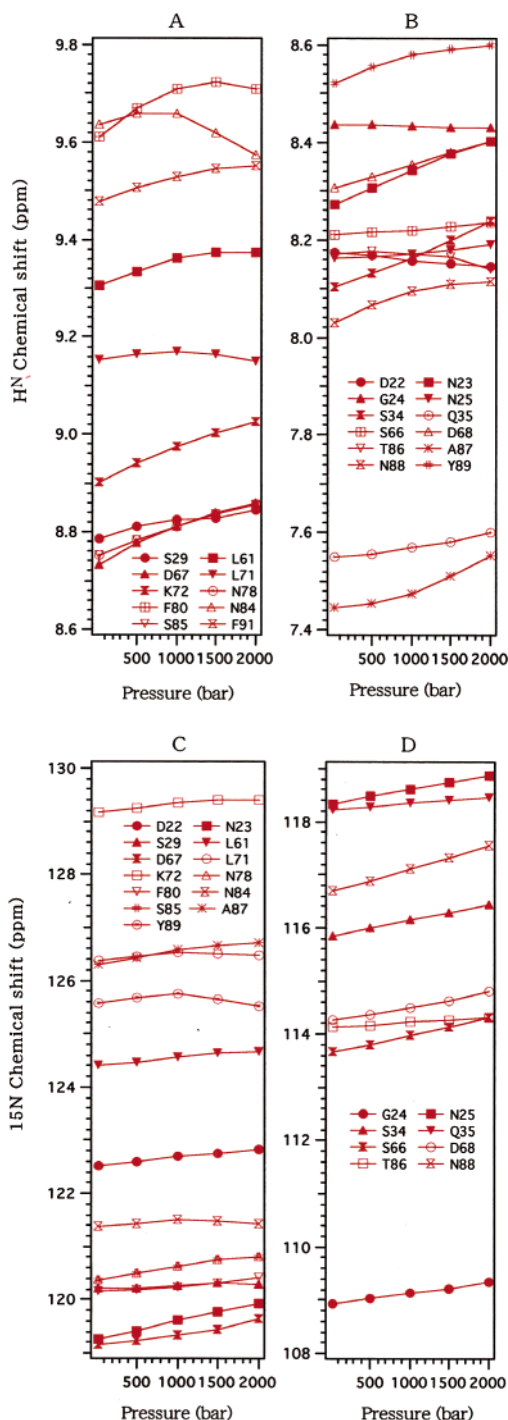


**Figure 10.** Plot of chemical shifts of selected amide protons ( $^1\text{H}$ ) (A and B) and amide nitrogens ( $^{15}\text{N}$ ) (C and D) of the Ras-binding domain of the Ral guanine nucleotide dissociation stimulator (Ral GDS) as a function of the pressure, showing distinct nonlinearity against pressure.<sup>62</sup> The experimental conditions are as follows: 1.2 mM  $^{15}\text{N}$ -labeled RalGDS-RBD, 15 mM Tris-HCl buffer, 150 mM NaCl, and 10 mM DTE at pH 7.3 and 25 °C.

water or the phenomena of fluorescence quenching of an internal Trp residue by external ions.

### 4.4. Fluctuation Involving Low-Lying Excited States (from Nonlinear Pressure Shifts)

The chemical shift is one of the most sensitive probes for pressure-induced conformational changes within the folded manifold for which  $^1\text{H}$  and  $^{15}\text{N}$  shifts can be followed for

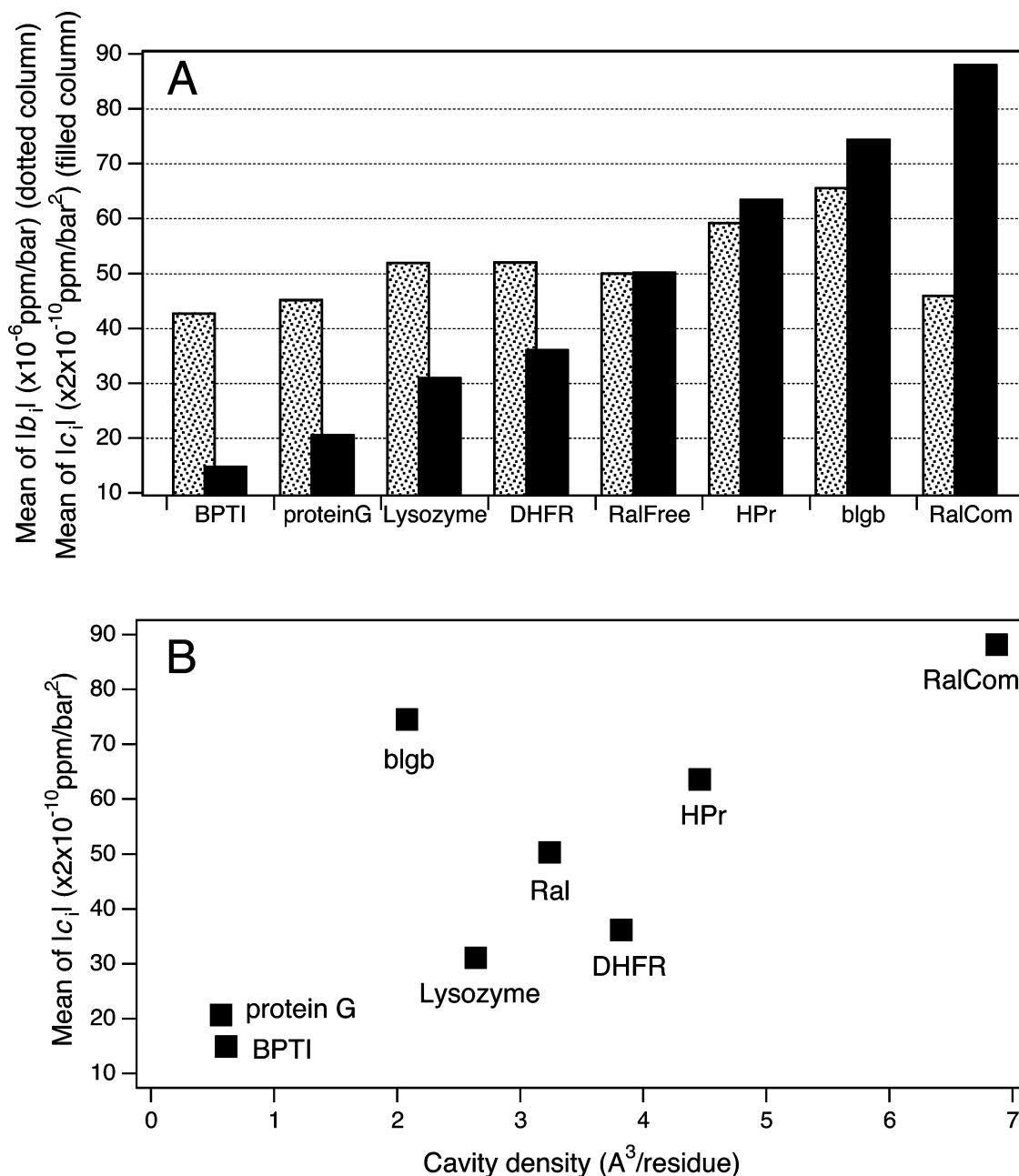


**Figure 11.** Nonlinearity–cavity relationship.<sup>62</sup> (A) Histograms of the mean of the absolute values of the second-order coefficient  $c_i$  (filled columns) and the first-order coefficient  $b_i$  (dotted columns) in eq 7 for  $^1\text{H N}$  in eight globular proteins. (B) Plot of the mean absolute values of the second-order coefficient  $c_i$  of  $^1\text{H N}$  pressure shifts versus the density of cavities (the total cavity volume divided by the number of amino acid residues) for the eight proteins. Cavity volumes of  $>20 \text{ \AA}^3$  are employed (calculated by GRASP using PDB coordinates). Note that the vertical scale for  $c_i$  is corrected from that of Figure 3 in ref 62.

individual amide groups (Figure 10). One of the interesting points here is that chemical shifts are quite linear for some proteins but distinctly nonlinear for other proteins.<sup>62</sup> An estimation of linearity and nonlinearity of chemical-shift changes with pressure is derived from least-squares fits of experimental data for individual  $^1\text{H}$  and  $^{15}\text{N}$  signals to the following equation

$$\delta_i = a_i + b_i p + c_i p^2 \quad (7)$$

where  $p$  is the pressure (bars),  $\delta_i$  is the chemical shift (parts per million) for the  $i$ th residue,  $a_i$  (parts per million) is the chemical shift at 1 bar, and  $b_i$  (parts per million per bar) and  $c_i$  (parts per million per square bars) are the first- and second-order coefficients in the pressure dependence of

chemical shifts.<sup>62</sup> In Figure 11A, averaged values of  $b_i$  and  $c_i$  are plotted for eight individual proteins. It shows that averaged absolute values of  $b_i$  (representing linear response to pressure, gray columns) do not vary much among different proteins but averaged absolute values of  $c_i$  (representing nonlinear response to pressure, black columns) vary enormously among proteins.

In Figure 11B, the averaged absolute values of the second-order coefficient  $c_i$  of  $^1\text{H N}$  pressure shifts are plotted against the density of cavities (larger than  $20 \text{ \AA}^3$ ) for the eight different proteins with a varying function from the protease inhibitor to signal-transaction protein. The excellent correlation seems to suggest that cavities large enough to hold water molecules are the major cause of nonlinearity with increasing pressure. The likely interpretation is that many proteins have

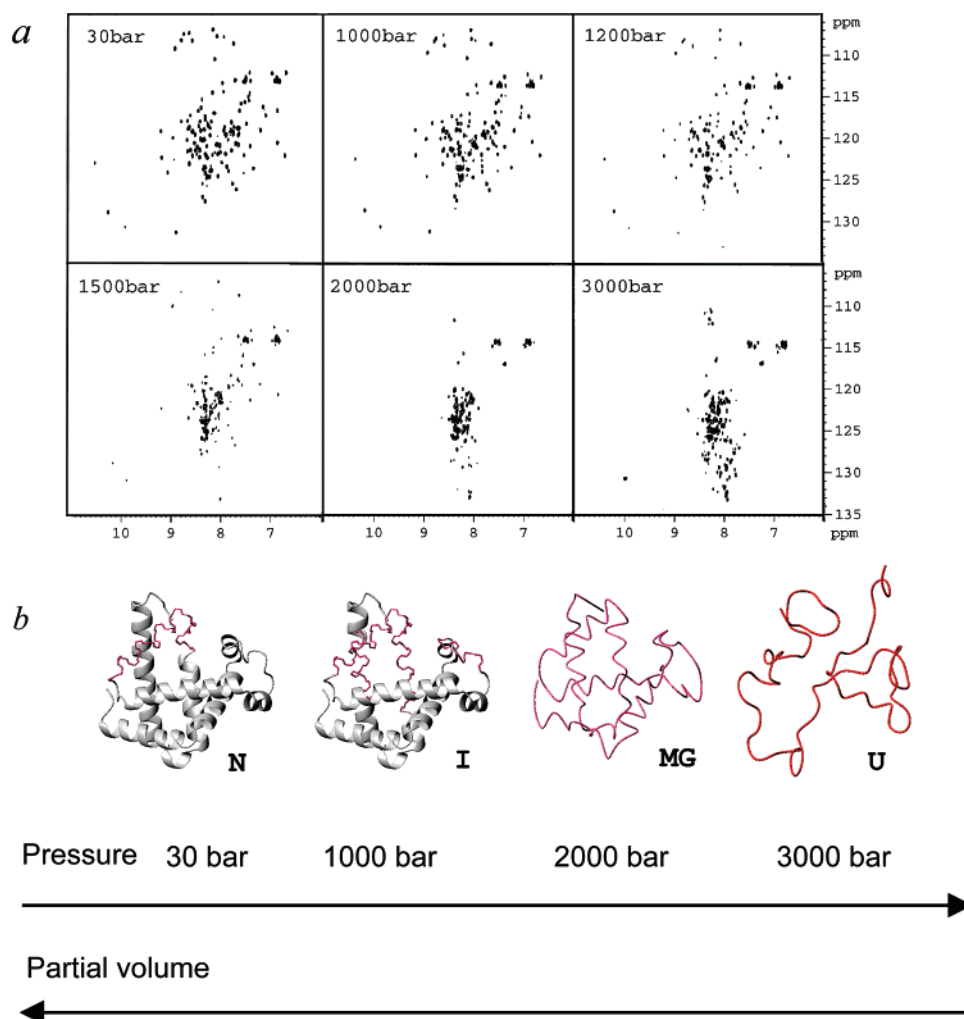


**Figure 12.** Illustration of the reversible conformational change of apomyoglobin with pressure. (a) Nearly reversible change of  $^{15}\text{N}/^1\text{H}$  HSQC spectra of  $^{15}\text{N}$ -uniformly labeled apomyoglobin. (b) Schematic representation of representative conformers dominant at various pressures. The thin lines represent disordered or unfolded regions of the polypeptide chain, while the ribbons represent the folded parts. Reprinted with permission from ref 63. Copyright 2002 Elsevier, The Netherlands.

low-lying excited states with partially hydrated cavities close to the level of the basic folded state and that these states are increasingly populated with increasing pressure because of their smaller partial molar volumes compared to that of the basic folded (ground) state. The limit of pressure to 2 kbar in Figure 10 fails to tell us whether the low-lying excited states form continuum or discrete levels for individual cases, although both cases are likely. One example for the presence of a discrete excited state conformer will be shown in section 5.5.

### 5. Probing Fluctuations Involving Transitions to Higher Energy Conformers

Larger conformational fluctuations leading to unfolding take place coupled with pressure and the negative  $\Delta V$  in eq 4. The use of pressure-coupled NMR experiments to probe protein unfolding has been pioneered with one-dimensional proton NMR by Jonas.<sup>8,9</sup> The recently developed NMR techniques, however, to monitor pressure effects on protein structure at kilobar ranges using two- or multidimensional NMR spectroscopy<sup>21,22,42,45</sup> have revolutionized the study of pressure effects on protein structure and dynamics to the full versatility of modern heteronuclear NMR spectroscopy.

#### 5.1. Probing Fluctuations in a Wider Conformational Space—The Underlying Principle

In many globular proteins, we find that as we apply pressure to the basic folded conformer, the  $^{15}\text{N}/^1\text{H}$  two-dimensional NMR spectrum undergoes a series of changes, showing that some intermediately folded conformers appear prior to full unfolding (Figure 12a). The analysis indicates that the protein undergoes conformational changes through a series of conformers, for example, N–I–MG–U in apomyoglobin, with increasing pressure<sup>63</sup> (Figure 12b). The N–I–MG–U sequence shows the decreasing order of conformation (i.e., tertiary structure). Through eq 4, the result suggests the notion that *the partial molar volume of a protein decreases in parallel with the decrease of the conformational order*. The generality of this notion has been confirmed experimentally in many globular proteins, leading us to call it the “volume theorem of protein”.<sup>63</sup> The theorem provides a guiding principle to experimentalists when exploring the multiple conformational nature of a globular protein with variable-pressure perturbation.

The decrease in volume upon a loss of conformational order may occur either by releasing intramolecular voids (i.e., cavities) or by contraction of the solvent near the newly

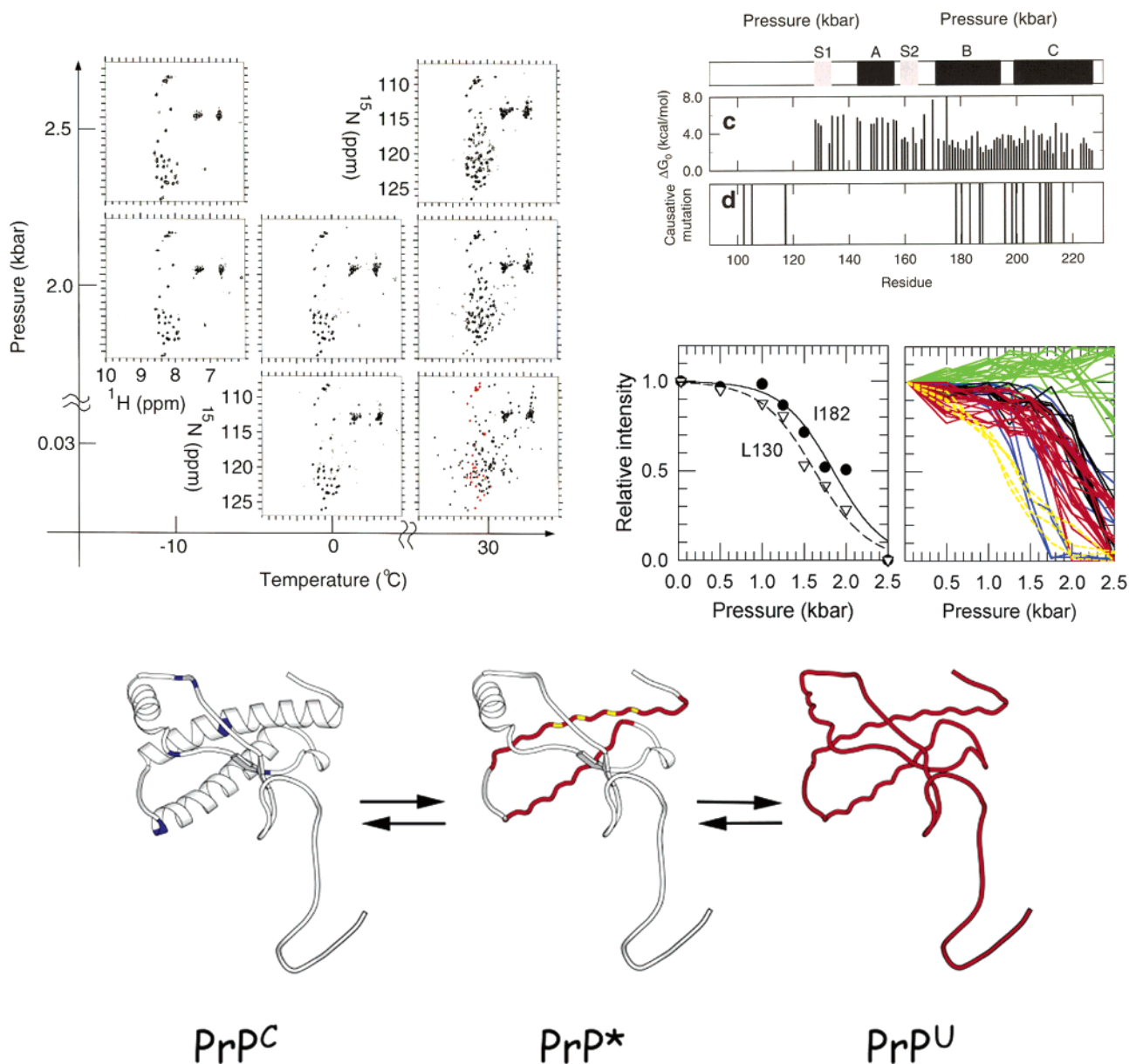


**Figure 13.** Conformational fluctuation in hamster prion.<sup>68</sup> (Upper left)  $^{15}\text{N}/^1\text{H}$  HSQC spectra as functions of the pressure and temperature. (Upper right) Stability of individual amide groups as a function of the pressure (a and b) and at 1 bar (c). Sites for causal mutations (d). (Below) Proposed conformational equilibrium of hamster prion (disordered regions are in red).

exposed protein surface. Both contributions are important, but the contribution of the latter is highly temperature-dependent and may change sign at high temperature. On the other hand, the former contribution is consistent over the temperature range of interest and is likely to play a significant part in the volume change ( $\Delta V$ ) of globular proteins.<sup>64</sup> The experimentally determined volume changes of unfolding for the mutants of *Staphylococcal* nuclease suggest that the loss of internal void volume upon unfolding represents the major contribution to the volume change ( $\Delta V$ ). A clear example was for the c-Myb R2 domain, in which filling a cavity by mutation dramatically decreased the volume change upon unfolding.<sup>65</sup> The significance of cavity contribution to the volume change ( $\Delta V$ ) has also been shown by statistical mechanical calculation of volume changes associated with the helix–coil transition.<sup>66</sup> Thus, the loss of the secondary and tertiary structures may both contribute to the loss of the volume of a globular protein.

## 5.2. Application to Globular Proteins

In many cases, excursion to a largely different conformer located higher in the energy landscape is slow on the NMR time scale, giving separate cross-peaks in the two-dimensional spectra such as  $^{15}\text{N}/^1\text{H}$  HSQC. In this case, elucidation of conformational stability can be made on the basis of the signal intensities of individual cross-peaks as a function of pressure, giving residue-specific  $\Delta G^\circ$  values by application of eqs 3 and 4. Often, a group of peaks decrease their intensities concertedly in a relatively low-pressure range, while the rest of the peaks remain intact, showing local denaturation or local unfolding.<sup>67</sup> In general, the pressure stabilities may differ among the individual cross-peaks, giving heterogeneous  $\Delta G^\circ$  values along the polypeptide chain. The resultant  $\Delta G^\circ$  values extrapolated to 1 bar for individual residues depict residue-specific stabilities at 1 bar.

An example is shown for hamster prion protein in Figure 13.<sup>68</sup> The lower stabilities of cross-peaks for selected regions

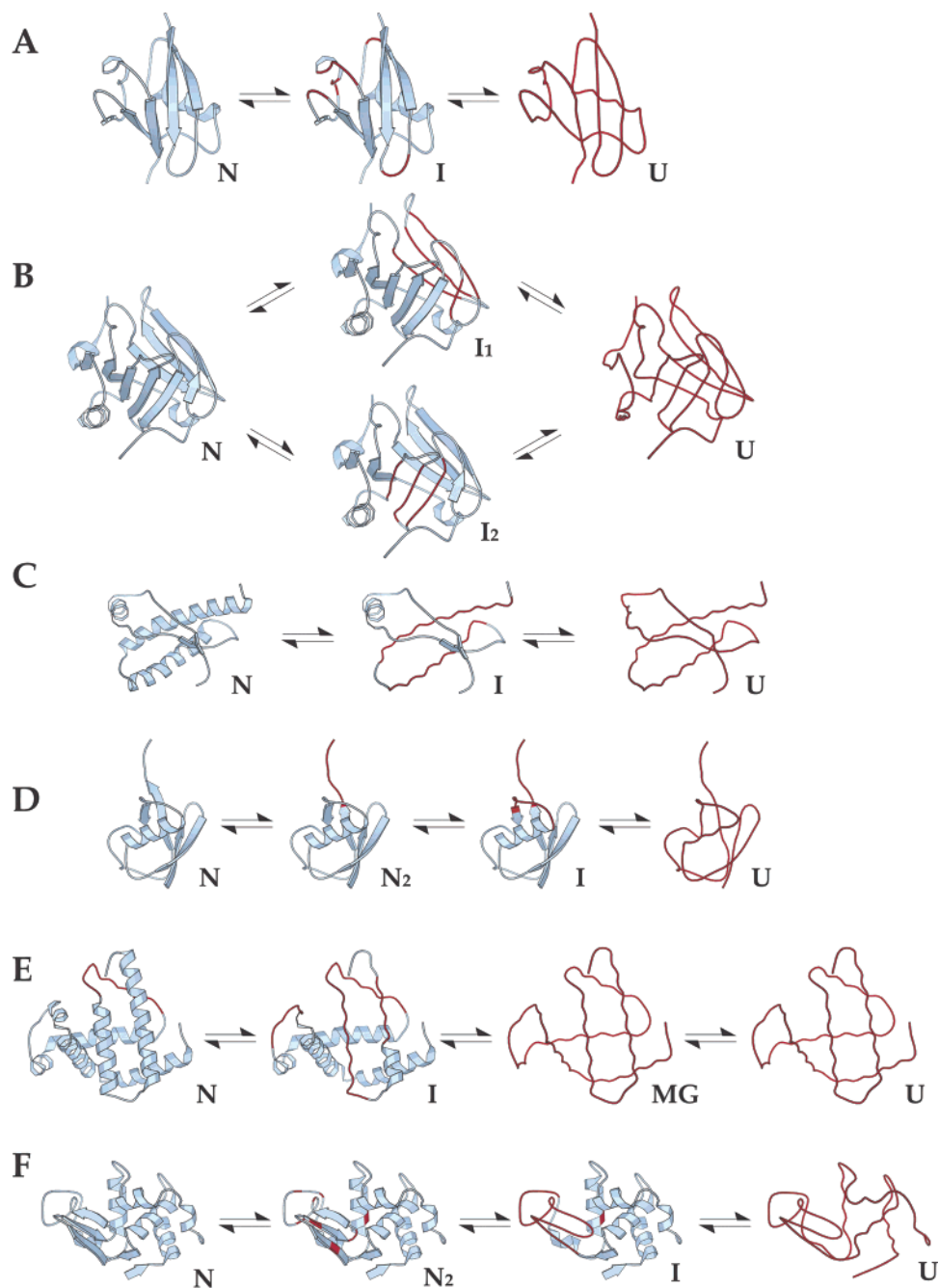


**Figure 14.** Conformational fluctuations in several globular proteins revealed from high-pressure NMR, which extends from N to U. Abbreviations: the basic folded conformer (N or  $N_1$ ), alternately folded conformer ( $N_2$ ), intermediate conformer (I), molten globule (MG), and totally unfolded conformer (U). Note that the structures of  $N_2$ , I, MG, and U are qualitatively drawn by representing the disordered/unstructured regions in thin red lines on the known basic folded structures (crystal structures). (A) Ras-binding domain of the Ral guanine nucleotide dissociation stimulator.<sup>67</sup> (B)  $\beta$ -Lactoglobulin.<sup>69</sup> (C) Syrian hamster prion protein rPrP(90–231).<sup>68</sup> (D) Ubiquitin.<sup>71</sup> (E) Sperm whale apomyoglobin.<sup>63</sup> (F) Hen lysozyme. Reprinted with permission from ref 73. Copyright 2004 Elsevier, The Netherlands.

of the molecule (red curves) are apparent, which correspond to the b and c helices. The result suggests that an intermediate conformer with local disorder in the b and c helices coexists at a population of  $\sim 1\%$  with the dominant folded conformer under physiological conditions (at 1 bar). Furthermore, the onset of complete unfolding at all residue sites is recognized at the extreme pressure (2.5 kbar), suggesting a coexistence of a much lower fraction of the fully unfolded conformer at 1 bar. This example shows that one can “scan” the entire allowed energy landscape of the hamster prion protein with high-pressure NMR by varying pressure within a relatively small range (from  $\sim 1$  to a few kbar).

Variable-pressure NMR experiments have been performed in many proteins including hamster prion,<sup>68</sup>  $\beta$ -lactoglobulin,<sup>69</sup> apomyoglobin,<sup>63</sup> P13<sup>MTCP1</sup>,<sup>70</sup> ubiquitin,<sup>71</sup> and dihydrofolate reductase,<sup>72</sup> most of which exhibit transitions to intermediate conformers (I,  $N_2$ , and/or MG) and further to totally unfolded conformers (U), some results of which are shown in Figure 14.<sup>73</sup> Note that all of the non-N structures depicted in Figure 14 are qualitative in that coordinates of N are used in which the unordered parts are colored. It is important to note that all of the transitions are reversible, implying that all of the structures are in equilibrium not only at high pressure but also at ambient pressure. These non-N conformers are hidden

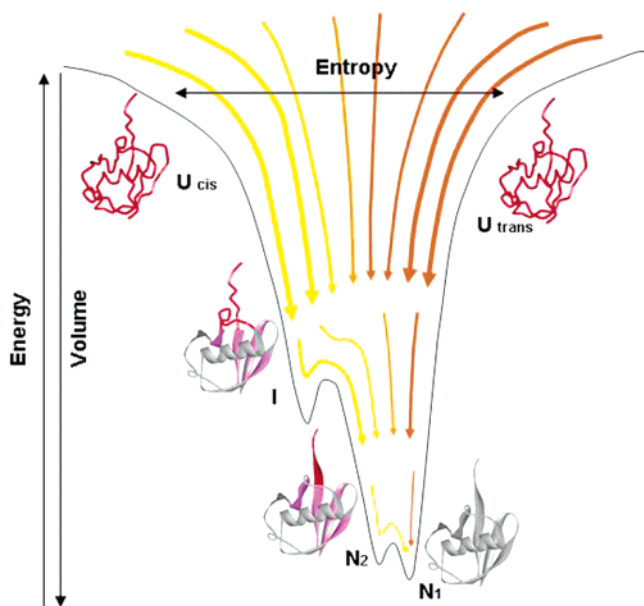


**Figure 15.** Conformational fluctuations of ubiquitin among conformers  $N_2$ , I, MG, and U (revealed by variable-pressure NMR<sup>71</sup>) expressed on the hypothetical energy landscape. The conformers detected by variable-pressure NMR are arranged in the order of decreasing conformational order as well as in partial molar volume:  $N_1 > N_2 > I > U$ . Ribbon model (in gray) for the folded part, ribbon model (in purple) for the distorted part, and wire model (in red) for the unfolded part.

at ambient pressure, but their presence is disclosed under variable pressure. They constitute an important component of the structural fluctuations of globular proteins and occur among substates differing in free energy. The uniqueness of their structures along with their populations suggests that they are likely the result of evolutionary pressure. If this hypothesis is correct, it should be crucially important to disclose their presence and characterize in detail their structures and populations under physiological conditions. Herein resides the utility of experiments on the pressure axis, particularly, that of variable-pressure NMR.

The conformational fluctuation involving different conformational order and energy can be best described using an energy landscape,<sup>74</sup> the vertical axis of which is parallel to the conformational order. In ubiquitin, Kitahara et al. studied structures and populations of all of the subensembles of conformers, N,  $N_1$ ,  $N_2$ , I, and U, by variable-pressure NMR. These conformers are placed in decreasing conformational order on the vertical axis of the hypothetical energy landscape in Figure 15, drawn for the condition (pH 4.5 and 0 °C). From the volume theorem, the vertical axis is considered parallel also to the partial molar volume of the protein.

The simultaneous use of pressure and temperature perturbations is often useful to extend the conformational space covered by the experiment. Because the freezing point of water is  $-21$  °C at 2 kbar, pressure can be used to observe cold denaturation of most proteins relatively easily if the low temperature range is utilized simultaneously with pressure perturbation. After the initiation by Jonas in hen lysozyme,<sup>75</sup> cold-induced denaturation has been used in several proteins, including prion,<sup>49</sup> HPr,<sup>58</sup> and ubiquitin,<sup>71</sup> to widen the conformational space covered.

A modest range of pressure (within a few tens of bars) has been used to prepare reverse micelles in low-viscosity

organic solvents,<sup>76</sup> with a purpose of extending the NMR study to higher molecular-weight proteins, which tend to tumble slowly. In this approach, a protein is encapsulated into the water cavity formed by a reversed micelle that in turn can be dissolved in nonpolar low-viscosity solvents such as propane and ethane. Using the same technique, the freezing point of water can be made even lower than  $-21$  °C, which may make it even easier to extend the conformational space of a protein available to spectroscopy, as shown for ubiquitin by Wand et al.<sup>77</sup>

### 5.3. Kinetic Studies Using Pressure

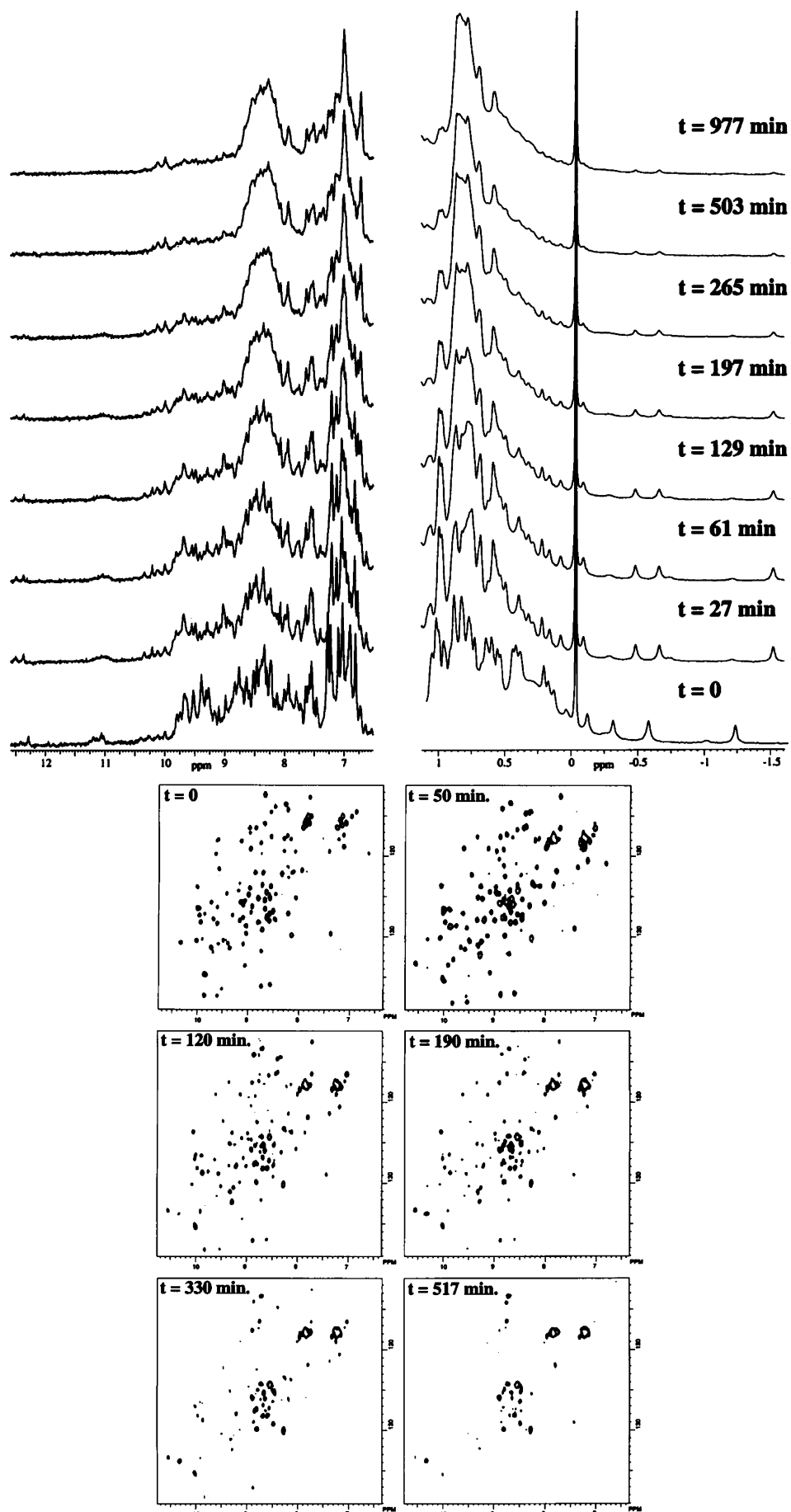
Information on transition states associated with conformational changes can only be obtained from kinetic experiments. In particular, *activation volume* is crucially important in assessing the conformation of a protein in the transition state, which can be obtained by kinetic experiments under variable pressure. To study the pressure effect on rapid folding kinetics (in  $\sim$ milli-seconds), one can perform stopped-flow measurements under variable pressure with fluorescence, infrared absorption, and X-ray scattering as monitor.<sup>78,79</sup> Folding or unfolding initiated by the pressure jump is another way to study the kinetic process of folding and unfolding.

One should note that a momentary temperature change results in a pressure jump because of adiabatic compression or expansion. For a two-state transition, however, this is avoided by carrying out small pressure jumps required to remain in the relaxation limit, giving only a small instantaneous change in temperature. Moreover, a common observation is that, while the unfolding and refolding transitions are quite fast (milli-second time scales) at atmospheric pressure, the relaxation profiles at high pressure often span time scales of minutes to hours. This is due to positive activation volumes for folding and/or unfolding reactions and allows for the use of NMR to monitor the pressure-induced folding or unfolding reaction with real time. Pressure-jump one- and two-dimensional NMR spectroscopy has been applied to study the unfolding of P13<sup>MTCPI</sup> (Figure 16),<sup>70</sup> which allows one to monitor the conformational transition at individual amino acid sites.

### 5.4. Close Identity of Kinetic Intermediates with Equilibrium Intermediates Stabilized by Pressure

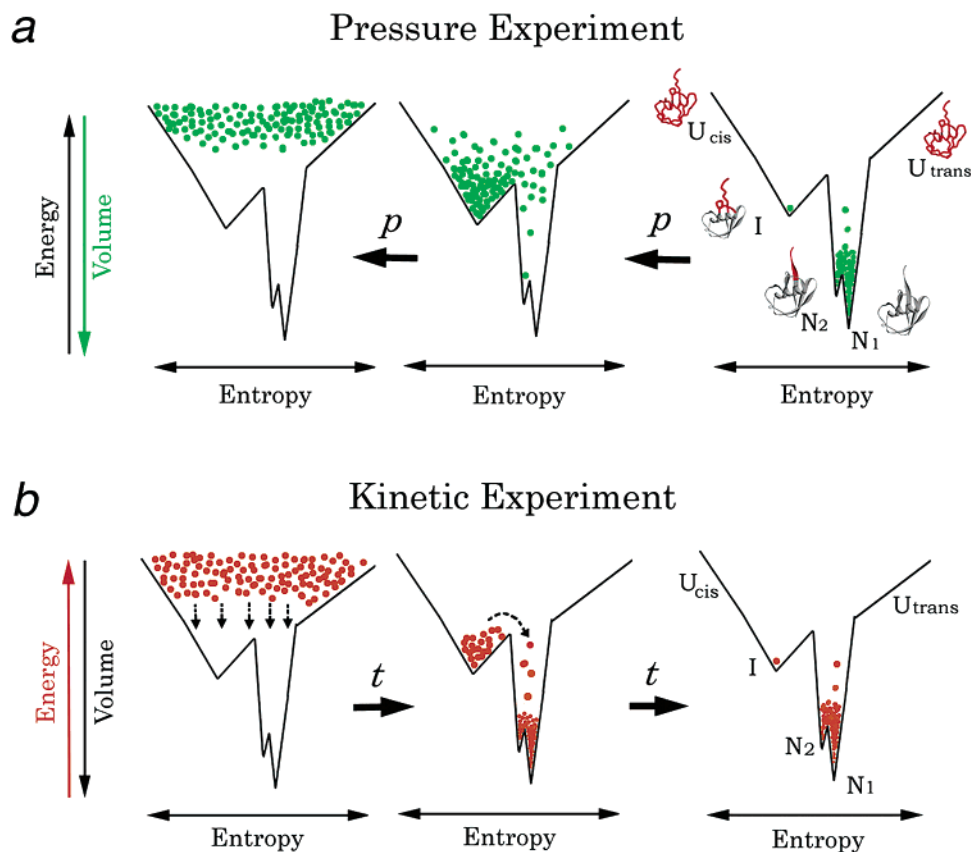
Our understanding of the result of high-pressure NMR like that given in Figure 14 is that a protein exists in solution fluctuating among different conformers from the basic folded conformer (frequently called N) and the totally unfolded conformer (U). In other words, the protein is undergoing folding and unfolding repeatedly even under physiological conditions at 1 bar. This concept immediately leads to the notion that the experiment with decreasing pressure mimics the folding process from U to N. The conformers appearing on the way from U to N may be considered to be folding intermediates.

Figure 17 shows schematically a folding funnel representing the entire available conformational space with ubiquitin at pH 4.5 and 20 °C as an example. The vertical axis of the funnel represents the free energy of a solvated single ubiquitin molecule (increasing upward), which also represents the conformational order of the polypeptide chain (increasing downward), whereas the horizontal scale represents the conformational entropy of ubiquitin.<sup>15</sup> A kinetic



**Figure 16.** Pressure-jump unfolding of P13MTCP1 monitored by one-dimensional  $^1\text{H}$  (top) and two-dimensional  $^{15}\text{N}/^1\text{H}$  HSQC (bottom) NMR spectral changes. Pressure was jumped from 30 bar to 3 kbar. Reproduced from ref 70.





**Figure 17.** Concept of the equilibrium pressure experiment (a) versus the concept of the kinetic-folding experiment (b), carried out under closely identical solution conditions.<sup>71</sup> The vertical axis of the funnel represents the internal energy of a hydrated protein molecule (increasing upward), i.e., a free energy of a single protein molecule, parallel to the conformational order of a polypeptide chain (increasing downward). The horizontal scale represents conformational entropy. The density of dots at each position in the funnel represents either the equilibrium population of the protein molecule under pressure (green) or a transiently occupying population at a certain time after commencement of the folding experiment (red). Protein structures are drawn with WebLab VIEWERLITE 3.2, with the red color representing highly disordered segments.

folding experiment is initiated by suddenly placing the entire ensemble of protein molecules close to the top of the folding funnel under the condition for folding (Figure 17b, far left). Then, the folding process is essentially a process of redistributing the ensemble over this basically funnel-shaped energy landscape. On average, molecules go downward on the funnel until an equilibrium population distribution is reached under the chosen condition. During this process, some molecules may be trapped transiently in a trough forming transient intermediates (Figure 17b, second from the left).

On the other hand, a variable-pressure experiment starts where the equilibrium population distribution is reached on the same landscape (Figure 17a, far right). Applying pressure under isothermal conditions is to redistribute the ensemble on the funnel until it reaches a new equilibrium of population defined by eq 3. A new equilibrium is reached at the applied pressure in favor of lower volume conformers mainly through the  $p\Delta V^\ddagger$  term of eq 4 under isothermal conditions. Because of the proposed parallelism between the volume and conformational order (the vertical axis of Figure 17), the new equilibrium would have a new population distribution on the funnel such that more populations are found on the upper part of the funnel, Figure 17a (middle), than in Figure 17a (right). In the limiting high pressure, the distribution may reach Figure 17a (left). In contrast to the kinetic experiment, in the equilibrium pressure experiment, intermediates can be trapped stably for any length of time (hours and even

days), thereby allowing two- or multidimensional NMR data acquisition necessary for detailed structural analysis of the trapped intermediates. It is to be emphasized that, in contrast to temperature and chemical perturbations such as pH or denaturants, which may completely alter the energy landscape and could even reverse the bottom against the top, perturbation by pressure is much more subtle energetically. This would leave the energy landscape much less altered, as schematically depicted in Figure 17a, in the variable-pressure experiment as long as we work in a relatively low-pressure range within a few kilobars. This makes the variable-pressure NMR a particularly useful technique to study structures of kinetic intermediates in protein folding in detail. The effect of pressure on the energy landscape of the protein, however, is still an open issue to be examined in detail, particularly with respect to the effect of hydration.

### 5.5. NMR "Snapshots" of a Fluctuating Protein Structure

In Figure 14, only qualitative structures are shown for all of the non-N structures in dynamic equilibrium with the basic folded conformer N, while the structures of N are expressed in the atomic coordinate by X-ray crystallography or NMR in solution. Is it possible to express the structures of non-N conformers also in atomic coordinates?

The high-pressure  $^{15}\text{N}/^1\text{H}$  (HSQC) two-dimensional NMR experiments carried out for ubiquitin at pH 4.6 and 20 °C in

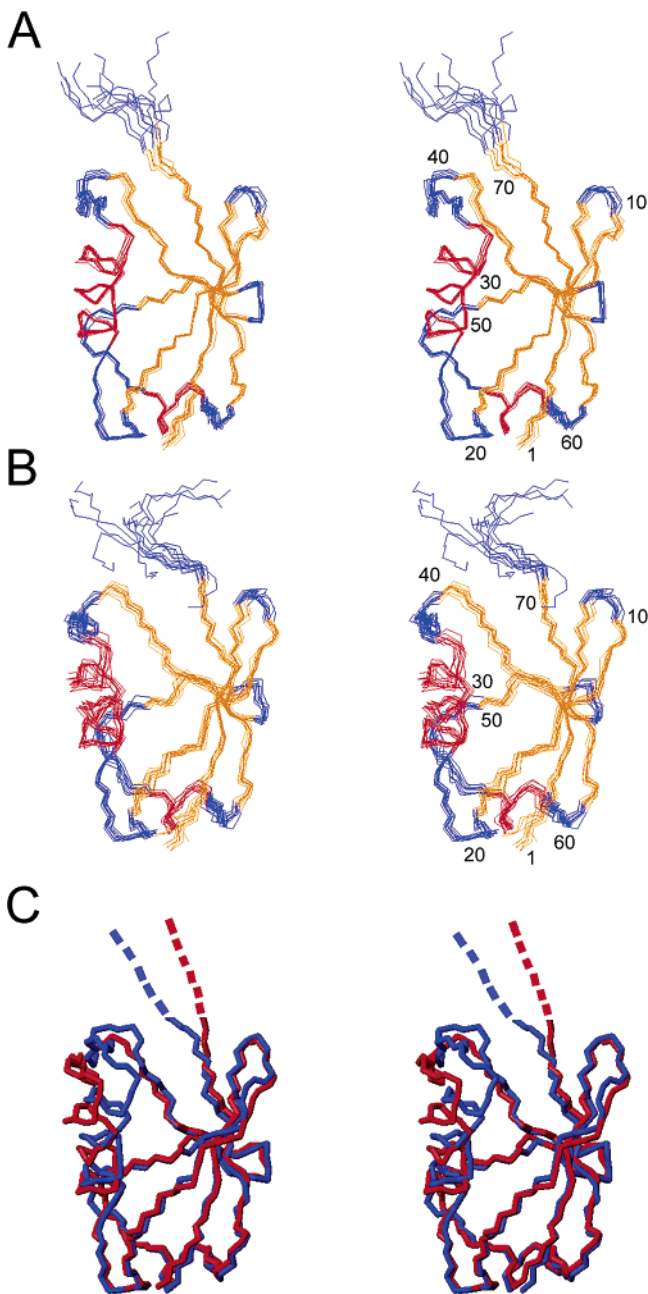


**Figure 18.** NMR snapshots (stereopairs) of fluctuating ubiquitin (pH 4.6 and 20 °C). (A) Snapshot at 30 bar (PDB accession number 1V80). (B) Snapshot at 3 kbar (PDB accession number 1V81). Both are shown in 10 energy-minimized structures ( $\alpha$  helices, red;  $\beta$  strands, yellow; others, blue). (C) Superposition of the snapshots at 30 bar (blue) and 3 kbar (red), each represented by an average of 10 convergent structures. Reprinted with permission from ref 80. Copyright 2005 Elsevier, The Netherlands.

a wide pressure range from 30 bar to 3.5 kbar showed large and reversible nonlinear  $^1\text{H}$  and  $^{15}\text{N}$  pressure shifts for several backbone amide groups (Figure 6).<sup>80</sup> A number of signals exhibit sigmoidal changes with pressure, depicting an overall two-state character of the transition. We have concluded that the protein exists in rapid ( $k_{12}, k_{21} \gg 10^3 \text{ s}^{-1}$ ) equilibrium between two major conformers  $N_1$  and  $N_2$ , namely



in which  $N_1$  is dominant at 1 bar ( $\sim 85\%$  calculated from the stability difference  $\Delta G^\circ$  of 4.2 kJ/mol), but  $N_2$  is more

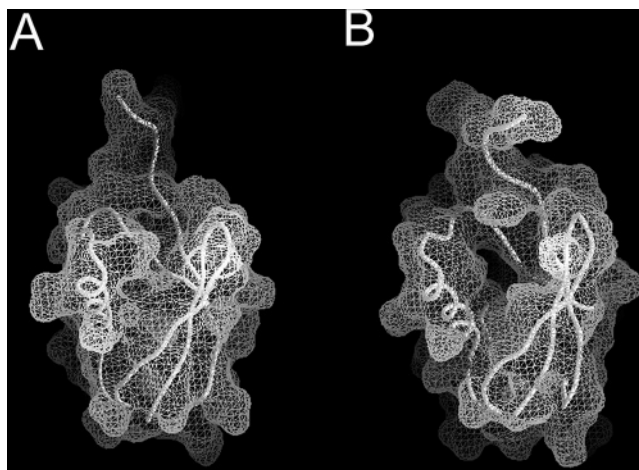


**Figure 19.** Molecular surface of ubiquitin at 30 bar (a) and 3 kbar (b), calculated for selected energy-minimized structures using GRASP with a probe radius of 1.4 Å. Reprinted with permission from ref 80. Copyright 2005 Elsevier, The Netherlands.

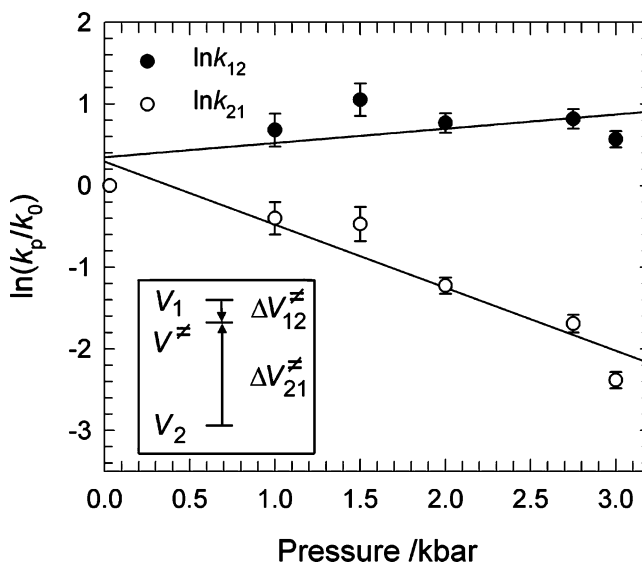


**Figure 20.** Experimentally determined rate constants  $k_{12}$  (●) and  $k_{21}$  (○) for the conformational transition between  $N_1$  and  $N_2$  (eq 8) as a function of the pressure. The symbols  $k_0$  and  $k_p$  represent the rate constant ( $k_{12}$  or  $k_{21}$ ) at 30 bar ( $k_{12} = 0.72 \times 10^5 \text{ s}^{-1}$ ,  $k_{21} = 4.12 \times 10^5 \text{ s}^{-1}$ ) and the rate constant at pressure  $p$ , respectively. The slopes give activation volumes  $\Delta V_{12}^\ddagger$  ( $-4.2 \pm 3.2 \text{ mL/mol}$ ) and  $\Delta V_{21}^\ddagger$  ( $18.5 \pm 3.0 \text{ mL/mol}$ ) for the transition from  $N_1$  to  $N_2$  and from  $N_2$  to  $N_1$  (defined in the inset), respectively. (Inset)  $V_1$ ,  $V_2$ , and  $V^\ddagger$  represent partial molar volumes of  $N_1$ ,  $N_2$ , and the transition-state conformer, respectively. Reprinted with permission from ref 80. Copyright 2005 Elsevier, The Netherlands.

populated at 3 kbar ( $\sim 77\%$ ) because of the smaller partial molar volume ( $\Delta V^\circ$  of  $-24 \text{ mL/mol}$ ). This demonstrates the case that a protein undergoes a large-scale motion between 2-folded conformers with distinctly different partial molar volumes and free energies (cf. Figure 15).

Can the structure of  $N_2$  be described in average coordinates? NMR experiments were performed for ubiquitin (10 mM at pH 4.6 and 20 °C) under pressure at 3 kbar as well as at 30 bar, and more than 1000 NOE distance constraints and more than 40 torsion angle constraints were obtained, which were used to calculate average coordinates at both pressures. The result reveals clearly a large difference in structures of ubiquitin at two pressures, with the helix swinging in and out by  $>3 \text{ \AA}$  with a simultaneous reorienta-

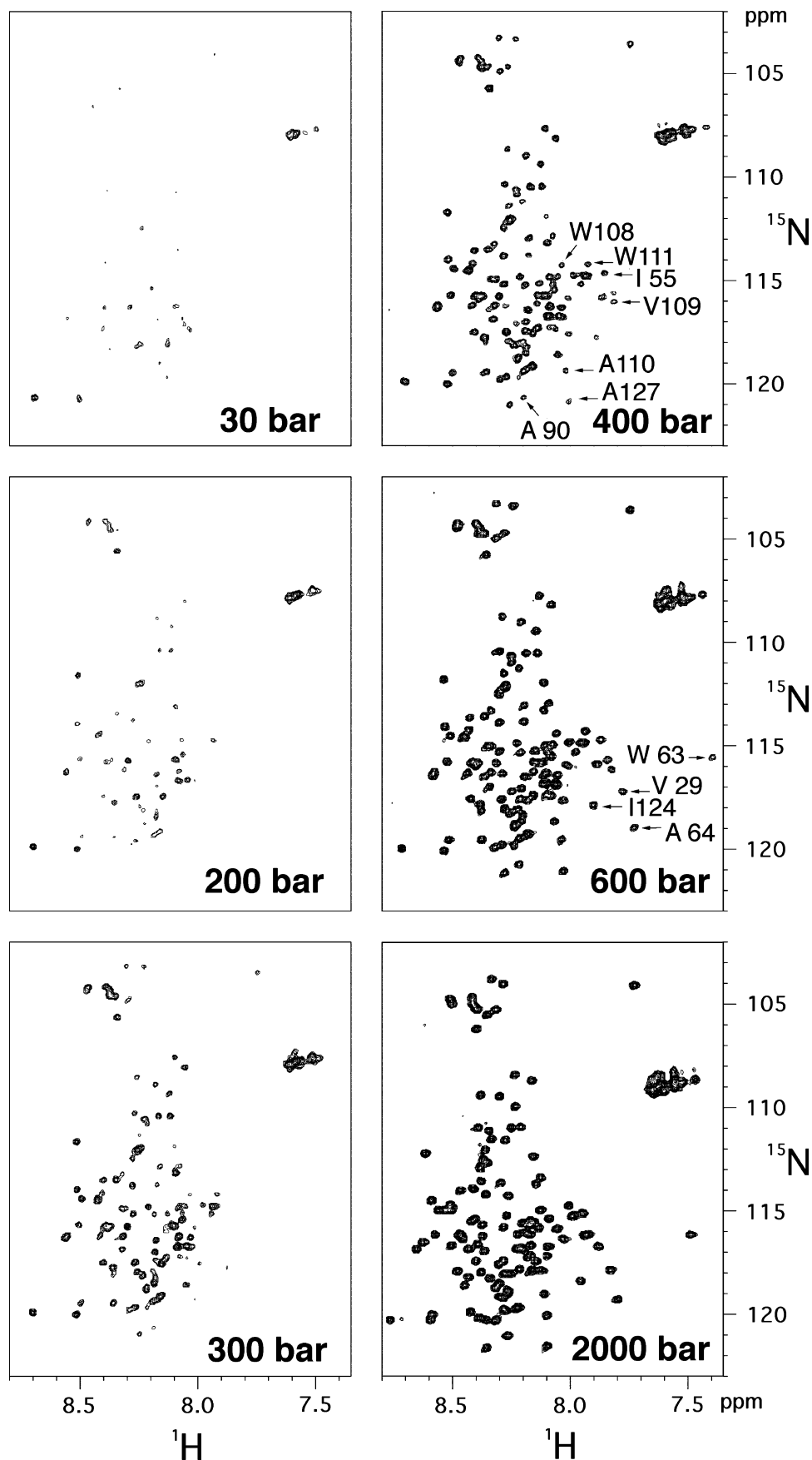


**Figure 21.** Self-assembly and pressure dissociation of disulfide-deficient hen lysozyme (OSS) monitored by  $^{15}\text{N}/^1\text{H}$  HSQC spectra. Dissociation and association can be repeated by pressurization at 2 kbar and depressurization at 1 bar. The assembly is formed in a time span of a day, and the equilibrium is characterized with a negative Gibbs energy for association of  $-23.3 \pm 0.8 \text{ kJ mol}^{-1}$  (in a monomer unit) and a positive volume change of  $52.7 \pm 11.3 \text{ mL mol}^{-1}$  (in a monomer unit) upon association. Reprinted with permission from ref 82. Copyright 2004 Elsevier, The Netherlands.

tion of the C-terminal segment. The structures at 30 bar and at 3 kbar are considered to closely represent two structures  $N_1$  and  $N_2$  of ubiquitin. The stereopairs shown in Figure 18 represent the first “NMR snapshots” of a fluctuating protein structure at atomic resolution.

Figure 19 shows the molecular surface of the protein at 30 bar (A) and at 3 kbar (B), as calculated by GRASP with a probe radius of 1.4 Å, and shows a partial opening of the core part and the increase of the molecular surface of the protein by about 5% at 3 kbar ( $\sim N_2$ ) relative to that at 30 bar ( $\sim N_1$ ). The previous observation of a significant decrease in partial molar volume ( $\Delta V^\circ = -24$  mL/mol) in going from the low-pressure conformer  $N_1$  to the high-pressure conformer  $N_2$  is totally consistent with the structural change depicted in Figure 18.

Although conformational fluctuations have been considered to be essential for protein function, visualization of actual shape changes for these fluctuations has seldom been performed experimentally. As seen above, pressure perturbation combined with NMR structure determination can achieve this goal. The method is general and can, in principle, be applied to any globular proteins, provided that the spectral resolution and the signal-to-noise ratio are sufficient. In essence, applying high pressure causes a shift of population from a higher volume (more ordered) conformer to a lower volume (less ordered) conformer. Likewise, lowering pressure causes a shift of the population from the lower volume conformer to the higher volume conformer. In other words, *pressure is used to amplify and trap the fluctuating conformer and NMR is used to analyze its structure in atomic detail.*

How fast is the fluctuation between  $N_1$  and  $N_2$ ? Transverse spin relaxation analysis showed that this fluctuation occurs in the 10  $\mu$ s time range and is pressure-dependent, with the activation volumes being  $-4.2 \pm 3.2$  and  $18.5 \pm 3.0$  mL/mol for the “closed-to-open” and the “open-to-closed” transitions, respectively (Figure 20). The difference ( $\Delta\Delta V^\ddagger = \Delta V_{12}^\ddagger - \Delta V_{21}^\ddagger = -22.7$  mL/mol) is consistent with the partial molar volume difference between the  $N_1$  and  $N_2$  conformers  $\Delta V_{21}^\circ (= -24$  mL/mol) determined previously from equilibrium experiments. The result shows that the transition state has a volume closer to  $N_1$ , whereas a relatively large volume increase ( $\Delta V_{21}^\ddagger = 18.5 \pm 3.0$  mL/mol) is required to reach the transition state from  $N_2$ . This is totally consistent with the open, hydrated character of the  $N_2$  conformer as depicted in Figure 19. The open surface in  $N_2$  might facilitate the interaction with enzymes by providing a binding platform for them. The large amplitude fluctuation depicted in Figure 18 is likely to be an intrinsic, evolutionarily selected property crucial for the function of ubiquitin.

## 6. Fluctuations Involving Self-Association

It has long been known that pressure leads to the dissociation of folded protein oligomers, with one good example being F actin.<sup>81</sup> More recently, the technique has been extended to the study of the self-assembly of denatured proteins, which are subjects of great interest in light of their relevance to aggregation of denatured proteins in general and specifically in amyloid fibril formation.

An intrinsically unfolded protein (U), represented by a disulfide-deficient variant (OSS) of hen lysozyme with no tertiary structure, self-assembles to a form rich in  $\beta$  structure under a mildly acidic condition containing NaCl.<sup>82</sup> The self-assembly turns out to be amyloid protofibrils, which grow

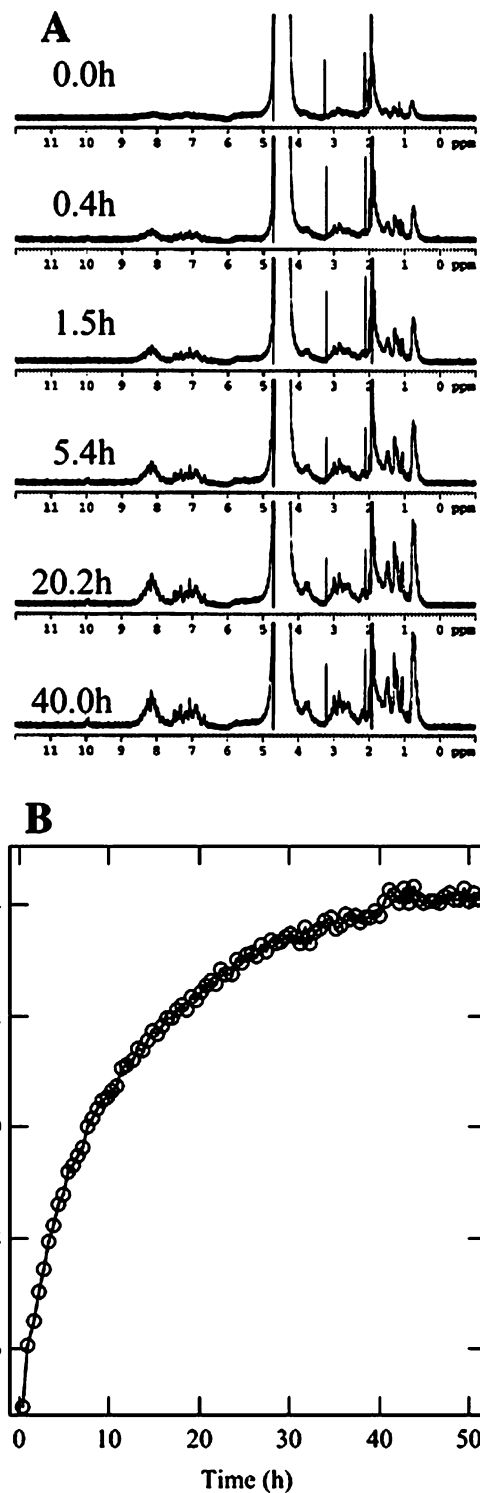


**Figure 22.** Time-dependent dissociation of disulfide-deficient hen lysozyme (OSS) by pressure at 2 kbar. (A) <sup>1</sup>H NMR spectra as a function of the time elapsed after application of 2 kbar of pressure. (B) Plot of the intensity of the methyl <sup>1</sup>H peak at  $\sim 0.9$  ppm against the time elapsed at 2 kbar of pressure. Reprinted with permission from ref 83. Copyright 2005 Elsevier, The Netherlands.

into long fibrils over several months. Interestingly, this assembly is found to undergo complete dissociation by pressure in the range of a few kilobars but reassociates at ambient pressure (Figure 21), showing that the self-assembly is in equilibrium with monomeric species and, therefore, that in a wide sense the association–dissociation phenomenon may also be considered to be part of the conformational fluctuation of this protein. For the assembly formed in a time

span of a day, the equilibrium is characterized with a negative Gibbs energy for association of  $-23.3 \pm 0.8 \text{ kJ mol}^{-1}$  (in a monomer unit) and a positive volume change of  $52.7 \pm 11.3 \text{ mL mol}^{-1}$  (in a monomer unit) upon association.

This result indicates that a seemingly irreversible aggregation reaction can be shown to be reversible and the thermodynamic parameters governing the equilibrium can be determined by using pressure as perturbation. Even the kinetics of the dissociation and association reaction can be studied relatively easily using pressure. Figure 22 shows the time-dependent dissociation process of the amyloid protofibrils of OSS on the  $^1\text{H}$  NMR spectrum upon a pressure jump from 30 bar to 2 kbar.<sup>83</sup> The reassociation process upon a pressure jump down can also be followed with the same technique.

## 7. Conclusion

Pressure represents an energetically mild perturbation compared to temperature and chemical changes and is quite effective in “amplifying” the intrinsic fluctuations in proteins by acting on the volumes of component conformers. Pressure perturbation reveals new information on protein fluctuations, including their structure, thermodynamics, and kinetics, which, collectively, are central to the modern understanding of protein dynamics. The combination of pressure perturbation with NMR has a special position in pressure studies of proteins, because of the extremely high spatial resolution attainable with modern multidimensional instrumentation and versatile pulse sequences. Pressure perturbation is particularly useful in sliding the spectroscopic observation window to reveal slow, rare, and large-amplitude motions that have hitherto been neglected, undetected, or overlooked in experiments based on other perturbations. Available information indicates that these rare motions can be crucially important in protein function and malfunction and are likely to be evolutionarily selected and encoded in the DNA.

## 8. Acknowledgment

I thank all of my excellent collaborators, the joint works with whom have made the foundation of this review. I also thank the reviewers for many constructive comments and suggestions for improving the manuscript, although I could not reply to them all. This work has been performed as a part of the activity of the JSPS Core-to-Core Program-Integrated Action Initiative (17009).

## 9. References

- Privalov, P. L.; Gill, S. J. *Adv. Protein Chem.* **1988**, *39*, 191.
- Kauzmann, W. *Nature* **1986**, *325*, 763.
- Bridgman, P. W. *J. Biol. Chem.* **1914**, *19*, 511.
- Suzuki, K. *Rev. Phys. Chem. Japan* **1960**, *29* (March).
- Weber, G.; Drickamer, H. G. *Q. Rev. Biophys.* **1983**, *16*, 89.
- Wagner, G. *FEBS Lett.* **1980**, *25*, 446.
- Morishima, I. *Curr. Perspect. High-Pressure Biol.* **1987**, 325.
- Jonas, J.; Jonas, A. *Annu. Rev. Biomol. Struct.* **1994**, *23*, 287.
- Royer, C. A.; Hinck, A. P.; Loh, S. N.; Prehoda, K. E.; Peng, X.; Jonas, J.; Markley, J. L. *Biochemistry* **1993**, *32*, 5222.
- Fuentes, E. J.; Wand, A. J. *Biochemistry* **1998**, *37*, 9877.
- Frauenfelder, H. et al. *J. Phys. Chem.* **1990**, *94*, 1024–1038.
- Jonas, J.; Ballard, L.; Nash, D. *Biophys. J.* **1998**, *75*, 445.
- Akasaka, K.; Yamada, H. *Methods Enzymol.* **1998**, *338*, 134.
- Jonas, J. *Biochim. Biophys. Acta* **2002**, *1595*, 145.
- Akasaka, K. *Biochemistry* **2003**, *42*, 10875.
- Akasaka, K. *Pure Appl. Chem.* **2003**, *75*, 927.
- Cooper, A. *Proc. Natl. Acad. Sci. U.S.A.* **1976**, *73*, 2740.
- Gekko, K.; Hasegawa, Y. *Biochemistry* **1986**, *25*, 6563.
- Kundrot, C. E.; Richards, F. M. *J. Mol. Biol.* **1986**, *193*, 157.
- Urayama, P.; Phillips, G. N., Jr.; Gruner, S. M. *Structure* **2002**, *10*, 51.
- Akasaka, K.; Tezuka, T.; Yamada, H. *J. Mol. Biol.* **1997**, *271*, 671.
- Li, H.; Yamada, H.; Akasaka, K. *Biochemistry* **1998**, *37*, 1167.
- Iwadate, M.; Asakura, T.; Dubovskii, P. V.; Yamada, H.; Akasaka, K.; Williamson, M. P. *J. Biomol. NMR* **2001**, *19*, 115.
- Refaee, M.; Tezuka, T.; Akasaka, K.; Williamson, M. P. *J. Mol. Biol.* **2003**, *327*, 857.
- Williamson, M. P.; Akasaka, K.; Refaee, M. *Protein Sci.* **2003**, *12*, 1971.
- Li, H.; Yamada, H.; Akasaka, K. *Biophys. J.* **1999**, *77*, 2801.
- Royer, C. *Biochim. Biophys. Acta* **2002**, *1595*, 201.
- Brandts, J. F.; Oliveira, R. J.; Westort, C. *Biochemistry* **1970**, *9*, 1038.
- Hawley, S. A. *Biochemistry* **1971**, *10*, 2436.
- Zipp, A.; Kauzmann, W. *Biochemistry* **1973**, *12*, 4217.
- Panick, G.; Vidugiris, G.; Malessa, R.; Rapp, G.; Winter, R.; Royer, C. *Biochemistry* **1999**, *38*, 4157.
- Lassalle, M. W.; Yamada, H.; Akasaka, K. *J. Mol. Biol.* **2000**, *298*, 293.
- Kharakoz, D. P. *Biophys. J.* **2000**, *79*, 511.
- Pin, S.; Royer, C. A. *Methods Enzymol.* **1994**, *232*, 42.
- Ruan, K.; Balny, C. *Biochim. Biophys. Acta* **2002**, *1595*, 94.
- Dzwolak, W.; Kato, M.; Taniguchi, Y. *Biochim. Biophys. Acta* **2002**, *1595*, 131.
- Meersman, F.; Smeller, L.; Heremans, K. *Biophys. J.* **2002**, *82*, 2635.
- Fujisawa, T.; Kato, M.; Inoko, Y. *Biochemistry* **1999**, *38*, 6411.
- Winter, R. *Biochim. Biophys. Acta* **2002**, *1595*, 160.
- Johnson, J. B.; Lamb, D. C.; Frauenfelder, H.; Muller, J. D.; McMahon, B.; Nienhaus, G. U.; Young, R. D. *Biophys. J.* **1996**, *71*, 1563.
- Hitchens, T. K.; Bryant, R. G. *Biochemistry* **1998**, *37*, 5878.
- Urbauer, J. L.; Ehnhardt, M. R.; Bieber, R. J.; Flynn, P. F.; Wand, J. A. *J. Am. Chem. Soc.* **1996**, *118*, 11329.
- Yamada, H.; Nishikawa, K.; Honda, M.; Shimura, T.; Akasaka, K.; Tabayashi, K. *Rev. Sci. Instrum.* **2001**, *72*, 1463.
- Arnold, M. R.; Kremer, W.; Luedemann, H.-D.; Kalbitzer, H. R. *Biophys. Chem.* **2002**, *96*, 129.
- Akasaka, K.; Yamada, H. *Methods Enzymol.* **2001**, *338*, 134.
- Lipari, G.; Szabo, A. *J. Am. Chem. Soc.* **1982**, *104*, 4546; *ibid* 4559.
- Sareth, S.; Li, H.; Yamada, H.; Woodward, C. K.; Akasaka, K. *FEBS Lett.* **2000**, *470*, 11.
- Orehov, V. Y.; Dubovskii, P. V.; Arseniev, A. S.; Yamada, H.; Akasaka, K. *J. Biol. NMR* **2000**, *17*, 257.
- Kuwata, K.; Kamatari, Y. O.; Akasaka, K.; James, T. L. *Biochemistry* **2004**, *43*, 4439.
- Kitahara, R.; Yokoyama, S.; Akasaka, K. *J. Mol. Biol.* **2005**, *347*, 277.
- Akasaka, K.; Li, H.; Yamada, H.; Li, R.; Thoresen, T.; Woodward, C. K. *Protein Sci.* **1999**, *8*, 1946.
- Kamatari, Y. O.; Yamada, H.; Akasaka, K.; Jones, J. A.; Dobson, C. M.; Smith, L. J. *Eur. J. Biochem.* **2001**, *268*, 1782.
- Wagner, G.; DeMarco, A.; Wüthrich, K. *Biophys. Struct. Mech.* **1976**, *2*, 139.
- Wagner, G. *FEBS Lett.* **1980**, *112*, 280.
- Wagner, G. *Q. Rev. Biophys.* **1983**, *16*, 1.
- Campbell, I. D.; Dobson, C. M.; Moore, G. R.; Perkins, S. J.; Williams, R. J. P. *FEBS Lett.* **1976**, *70*, 96.
- Campbell, I. D.; Dobson, C. M.; Williams, R. J. *Proc. R. Soc. London, Ser. B* **1975**, *189*, 503.
- Hattori, M.; Li, H.; Yamada, H.; Akasaka, K.; Hengstenberg, W.; Gronwald, W.; Kalbitzer, H.-R. *Protein Sci.* **2004**, *13*, 3104.
- Kocher, J. P.; Prevost, M.; Wodak, S. J.; Lee, B. *Structure* **1996**, *4*, 1517.
- Lumry, R.; Rosenberg, A. *Coll. Int. CNRS L'Eau. Syst. Biol.* **1975**, *246*, 55.
- Pain, R. H. *Nature* **1987**, *326*, 247.
- Akasaka, K.; Li, H. *Biochemistry* **2001**, *40*, 8665.
- Kitahara, R.; Yamada, H.; Akasaka, K.; Wright, P. E. *J. Mol. Biol.* **2002**, *320*, 311.
- Gediminas, J.; Vidugiris, A.; Royer, C. A. *Biophys. J.* **1998**, *75*, 463.
- Lassalle, M. W.; Yamada, H.; Morii, H.; Ogata, K.; Sarai, A.; Akasaka, K. *Proteins: Struct., Funct., Genet.* **2001**, *45*, 96.
- Imai, T.; Harano, Y.; Kovalenko, A.; Hirata, F. *Biopolymers* **2001**, *59*, 512.
- Inoue, K.; Yamada, H.; Akasaka, K.; Herrmann, C.; Kremer, W.; Maurer, T.; Doeker, R.; Kalbitzer, H.-R. *Nat. Struct. Biol.* **2000**, *7*, 547.
- Kuwata, K.; Li, H.; Yamada, H.; Legname, G.; Prusiner, S. B.; Akasaka, K.; James, T. L. *Biochemistry* **2002**, *41*, 12277.

- (69) Kuwata, K.; Li, H.; Yamada, H.; Batt, C. A.; Goto, Y.; Akasaka, K. *J. Mol. Biol.* **2001**, *305*, 1073.
- (70) Kitahara, R.; Royer, C. A.; Yamada, H.; Boyer, M.; Saldana, J. L.; Akasaka, K.; Roumestand, C. *J. Mol. Biol.* **2002**, *329*, 609.
- (71) Kitahara, R.; Akasaka, K. *Proc. Natl. Acad. Sci. U.S.A.* **2003**, *100*, 3167.
- (72) Kitahara, R.; Sareth, S.; Yamada, H.; Ohmae, F.; Gekko, K.; Akasaka, K. *Biochemistry* **2000**, *39*, 12789.
- (73) Kamatari, Y. O.; Kitahara, R.; Yamada, H.; Yokoyama, S.; Akasaka, K. *Methods* **2004**, *34*, 133.
- (74) Frauenfelder, H.; Sligar, S. G.; Wolynes, P. G. *Science* **1991**, *254*, 1598.
- (75) Nash, D. P.; Jonas, J. *Biochemistry* **1997**, *36*, 14375.
- (76) Wand, A. J.; Ehrhardt, M. R.; Flynn, P. F. *Proc. Natl. Acad. Sci. U.S.A.* **1998**, *95*, 15299.
- (77) Babu, C. R.; Hilser, V. J.; Wand, A. J. *Nat. Struct. Mol. Biol.* **2004**, *11*, 352.
- (78) Desai, G.; Panick, G.; Zein, M.; Winter, R.; Royer, C. A. *J. Mol. Biol.* **1999**, *288*, 461.
- (79) Woenckhaus, J.; Kohling, R.; Thiyagarajan, P.; Littrell, K. C.; Seifert, S.; Royer, C. A.; Winter, R. *Biophys. J.* **2001**, *80*, 1518.
- (80) Kitahara, R.; Yokoyama, S.; Akasaka, K. *J. Mol. Biol.* **2005**, *347*, 277.
- (81) Ikai, T.; Ooi, T. *Biochemistry* **1966**, *5*, 1551.
- (82) Niraula, T. N.; Konno, T.; Li, H.; Yamada, H.; Akasaka, K.; Tachibana, H. *Proc. Natl. Acad. Sci. U.S.A.* **2004**, *101*, 4089.
- (83) Kamatari, Y. O.; Yokoyama, S.; Tachibana, H.; Akasaka, K. *J. Mol. Biol.* **2005**, *349*, 916.

CR040440Z